Continuum Percolation and Duality with Hard-Particle Systems Across Dimensions

Salvatore Torquato

Department of Chemistry

Department of Physics,

Program in Applied & Computational Mathematics,

& Princeton Institute for the Science and Technology of Materials

Princeton University

Clustering and Percolation

- The study of clustering behavior of particles in condensed-phase systems is of importance in a wide variety of phenomena:
  - nucleation
  - condensation of gases
  - gelation and polymerization
  - chemical association
  - structure of liquids
  - metal-insulator transition in liquid metals
  - conduction in dispersions
  - aggregation of colloids
  - flow in porous media
  - spread of diseases
  - wireless communication

Clustering and Percolation

- The study of clustering behavior of particles in condensed-phase systems is of importance in a wide variety of phenomena:
  - nucleation
  - condensation of gases
  - gelation and polymerization
  - chemical association
  - structure of liquids
  - metal-insulator transition in liquid metals
  - conduction in dispersions
  - aggregation of colloids
  - flow in porous media
  - spread of diseases
  - wireless communication

- Cluster ≡ a connected group of elements (e.g., sites or bonds in lattice or particles).
- Roughly speaking, as finite-sized clusters grow, the percolation threshold of the system, is the density at which a cluster first spans the system (long-range connectivity). In the thermodynamic limit, the percolation threshold is the point at which a cluster becomes infinite in size.
- Percolation theory provides a powerful means of understanding such clustering phenomena.

Overlapping Hyperspheres and Oriented Hypercubes

- **Prototypical continuum (off-lattice) percolation model: Equal-sized overlapping (Poisson distributed) hyperparticles in $\mathbb{R}^d$.**

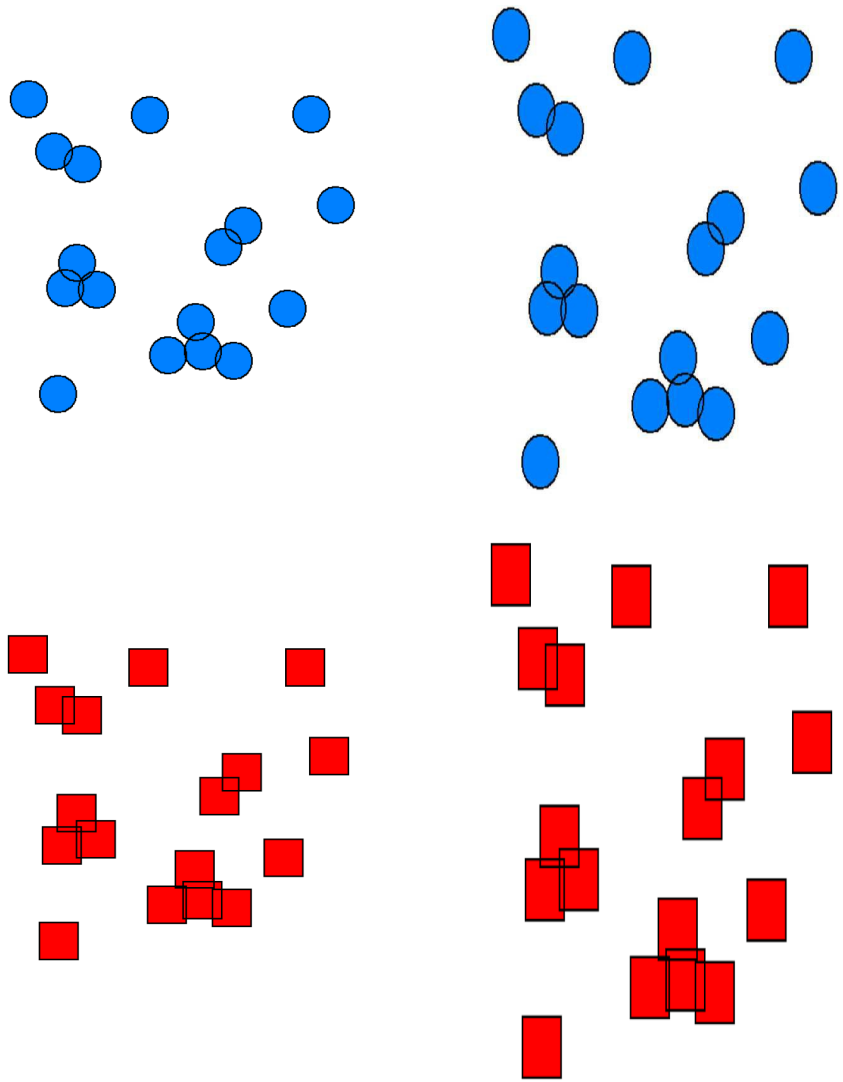

S. Torquato, "Effect of dimensionality on the continuum percolation of overlapping hyperspheres and hypercubes," Journal of Chemical Physics, 136, 054106 (2012).

Basic Definitions

- Consider equal-sized overlapping hyperspheres of diameter D in R^d at number density ρ and define the reduced density η by

$$\eta = \rho v_1(D/2), \tag{1}$$

where $v_1(R)$ is the d-dimensional volume of a sphere of radius R given by

$$v_1(R) = \frac{\pi^{d/2} R^d}{\Gamma(1 + d/2)}. \tag{2}$$

- For hypercubes of edge length D, $v_1(D/2) = D^d$.
- Fraction of space covered by the overlapping particles is

$$\varphi = 1 - \exp(-\eta). \tag{3}$$

- Two spheres of radius $D/2$ are considered to be connected if they overlap. Define the indicator function for the exclusion region as

$$f(r) = \begin{cases} 0, & r > D, \\ 1, & r \leq D \end{cases} \tag{4}$$

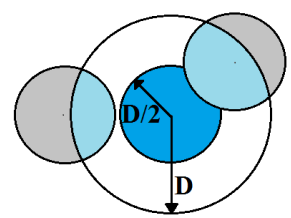

The volume of the exclusion region $v_1(D)$ is given by the volume integral of $f(r)$, i.e.,

$$v_1(D) = \int_{\mathrm{R}^d} f(r)\,dr = 2^d v_1(D/2). \tag{5}$$

- Mean number of overlaps per sphere N is given by

$$\mathrm{N} = \rho v_1(D) = 2^d \eta. \tag{6}$$

3D Hard Spheres in Equilibrium

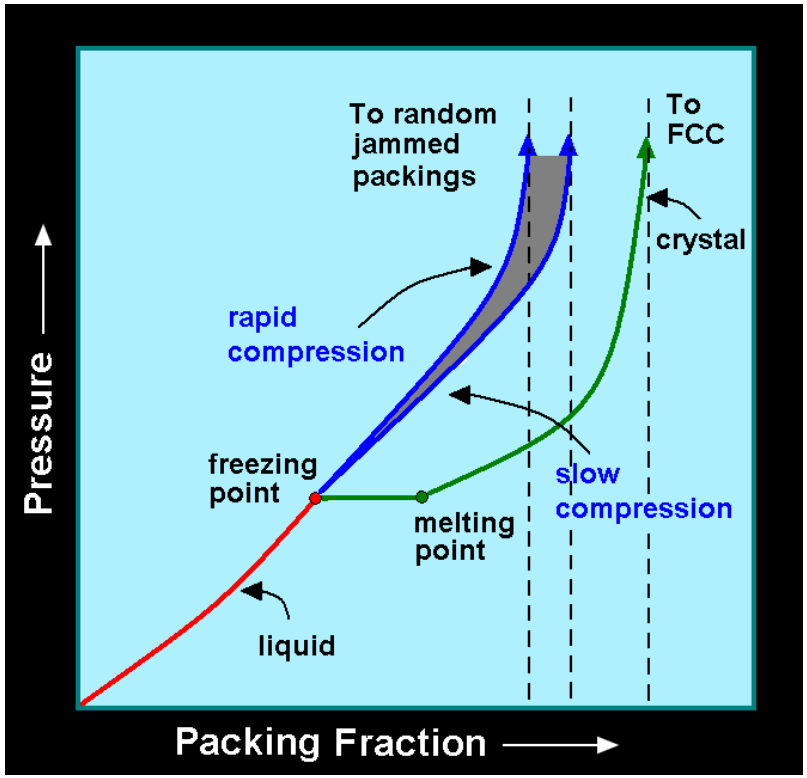

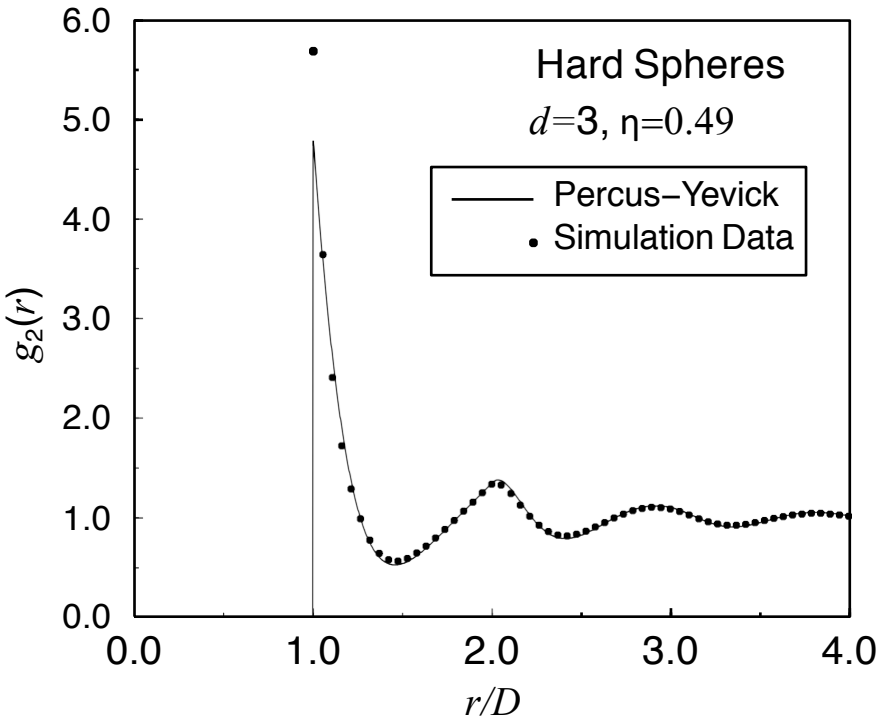

3D Hard Spheres in Equilibrium

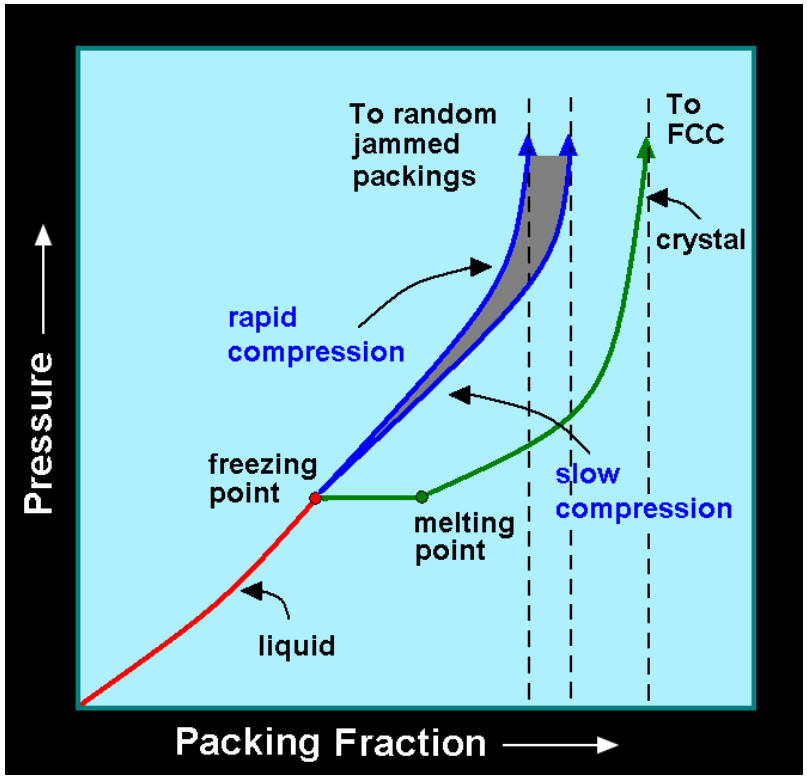

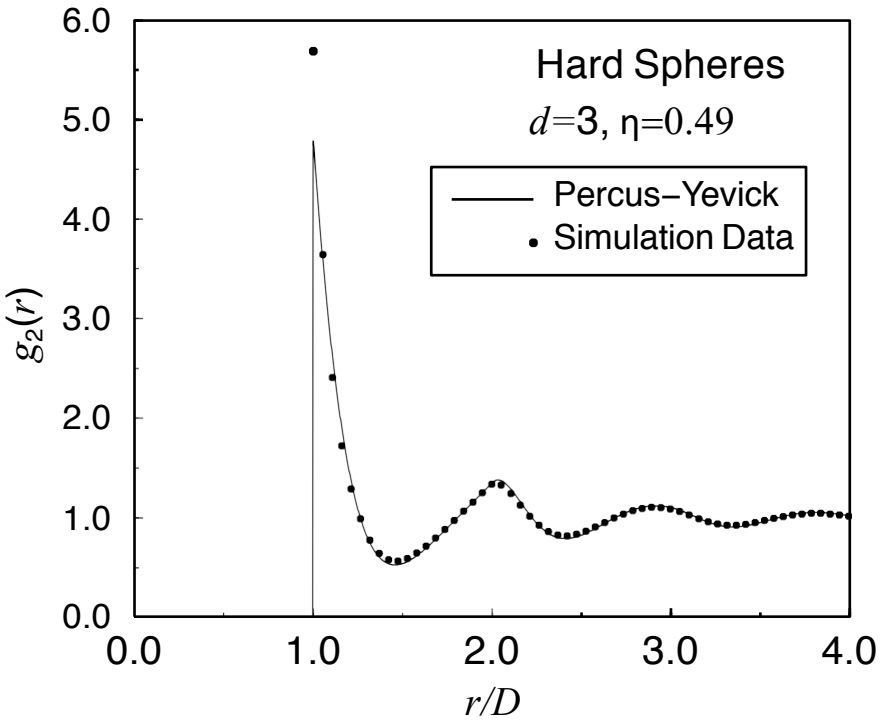

Still Many Theoretical Conundrums

- Do not know radius of convergence of virial expansion for p.
- No rigorous proof there is a first-order phase transition.
- No rigorous proof that FCC is the maximal density state.
- Are densest packings in high d disordered?

Definitions and Background

- The **pair-connectedness function** $P(\mathbf{r})$ is defined such that $\rho^2 P(\mathbf{r})\, d\mathbf{r}_1\, d\mathbf{r}_2$ is the probability finding any pair of particles of the same cluster in the volume elements $d\mathbf{r}_1$ and $d\mathbf{r}_2$ centered on $\mathbf{r}_1$ and $\mathbf{r}_2$, respectively, where $\mathbf{r} = \mathbf{r}_2 - \mathbf{r}_1$.

- **Mean cluster number** S is the average number of particles in the cluster containing a randomly chosen particle:

$$S = 1 + \rho \int_{\mathbb{R}^d} P(\mathbf{r})\, d\mathbf{r}. \tag{7}$$

- Since $P(\mathbf{r})$ becomes **long-ranged** at the **percolation threshold** η_c, it follows from (7) that S **diverges to infinity** as $\eta \to \eta_c^-$.

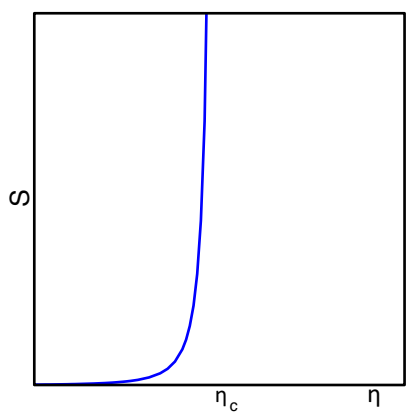

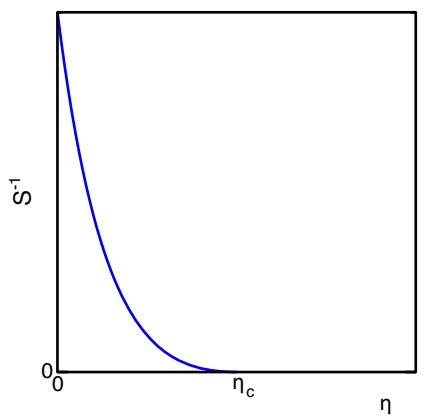

- It is believed that

$$S \propto (\eta_c - \eta)^{-\gamma}, \qquad \eta \to \eta_c^- \tag{8}$$

where γ is a **universal exponent** for a large class of lattice and continuum percolation models in dimension d. For example, $\gamma = 43/18$ for $d = 2$ and $\gamma = 1.8$ for $d = 3$. For $d \geq 6$, γ takes its dimension-independent **mean-field** value: $\gamma = 1$.

Results

- Show analytically that the $[0, 1]$, $[1, 1]$ and $[2, 1]$ Padé approximants of low-density expansion of S are upper bounds on S for all d.

- These results lead to lower bounds on η_c, which become progressively tighter as d increases and exact asymptotically as $d \to \infty$, i.e.,

$$\eta_c \to \frac{1}{2^d}$$

- Analysis is aided by a remarkable duality between the equilibrium hard-hypersphere (hypercube) fluid system and the continuum percolation model of overlapping hyperspheres (hypercubes).

topology $\Leftrightarrow$ geometry

- Show as d increases, finite-sized clusters become more ramified (branch-like).

- Analysis sheds light on the radius of convergence of density expansion for S and leads to an analytical approximation for η_c that applies across all d.

- Low-dimensional results encode high-dimensional information.

- Analytical estimates are used to assess previous simulation results for η_c up to twenty dimensions.

- Describe the extension of our results to the case of overlapping particles of general anisotropic shape in d dimensions with arbitrary orientations.

Ornstein-Zernike Formalism

Coniglio et al. (1977) derived the density expansion of $P(r)$ in terms of f : collection of diagrams having at least one unbroken path of f -bonds connecting root points 1 and 2, which can be divided into direct diagrams denoted by $C(r)$, direct connectedness function, and indirect diagrams:

$$P(r) = C(r) + \rho C(r) \otimes P(r),$$

where $\otimes$ denotes a convolution integral. Taking the Fourier transform of (8) gives

$$\tilde{P}(k) = \frac{\tilde{C}(k)}{1 - \rho \tilde{C}(k)}.$$

Therefore,

$$S = 1 + \rho \tilde{P}(0) \quad \text{or} \quad S^{-1} = 1 - \rho \tilde{C}(0),$$

which gives the critical percolation density to be

$$\eta_c = v_1(D/2)[\tilde{C}(0)]^{-1} = v_1(D/2) \left[\int C(r)dr \right]^{-1}. \tag{9}$$

The density expansions of the mean cluster number and its inverse are respectively

$$S = 1 + \sum_{m=1} S_{m+1} \eta^m \tag{10}$$

$$S^{-1} = 1 - \rho \int_{\mathrm{R}^d} C(\mathrm{r})dr = 1 - \sum_{m=1} C_{m+1} \eta^m. \tag{11}$$

where

$$S_m = \sum_{j=2}^{m} C_j S_{m+1-j}, \tag{12}$$

Overlapping Hyperspheres and Oriented Hypercubes

$$C(r) = \sum_{n=2} \rho^{n-2} c_n(r). \tag{13}$$

The first three terms of this series expansion have the following diagrammatic representations:

$c_2(r) =$ 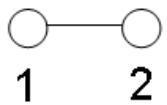

. (14)

$\rho\, c_3(r) = -$ 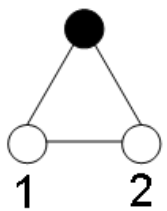

. (15)

$\rho^2\, c_4(r) = -$ 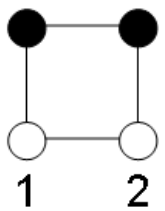

$+2$ 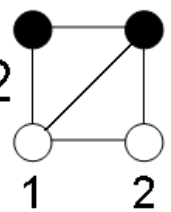

$+\frac{1}{2}$ 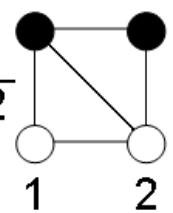

(16)

$-\frac{1}{2}$ 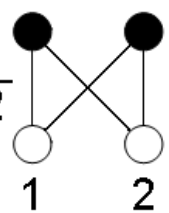

$+$ 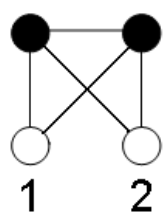

$-$ 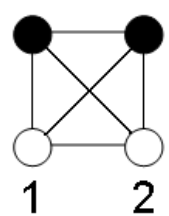

Dimer, Trimer and Tetramer Statistics

- **Dimer and trimer contributions, are respectively given by**

$$C_2 = \frac{1}{v_1(D/2)} \int_{\mathbb{R}^d} f(\mathbf{r})d\mathbf{r} = \frac{2B_2}{v_1(D/2)} = 2^d,$$

$$C_3 = -\frac{1}{v_1^2(D/2)} \int_{\mathbb{R}^d} f(\mathbf{r})v_2^{int}(\mathbf{r};D)d\mathbf{r} = -\frac{3\cdot B_3}{v_1(D/2)^2},$$

where

$$v_2^{int}(\mathbf{r};D) = f(\mathbf{r}) \otimes f(\mathbf{r})$$

is the intersection volume of two exclusion regions whose centroids are separated by the displacement vector $\mathbf{r}$, which is known analytically for any d.

- **The virial coefficient B_m is defined via the equation for the pressure p of a hard-particle system at number density ρ and temperature T, i.e.,**

$$\frac{p}{\rho k_B T} = 1 + \sum_{m=1}^{\infty} B_{m+1}\rho^m.$$

- **The tetramer contribution to the series expansion for $C(r)$:**

$$C_4 = -\frac{3}{2}C_4^A + \frac{7}{2}C_4^B - C_4^C,$$

B_4 for corresponding hard-particle system is also obtained from the sum of the diagrams corresponding to C_4^A, C_4^B and C_4^C but with weights $-3/8$, $3/4$ and $-1/8$.

Trimer Statistics

- $|C_3|/C_2^2$ is the probability that the pair of particles 2 and 3 are connected to one another given that particles 2 and 3 are each connected to particle 1.
- This conditional probability can be evaluated exactly as a function of dimension for both overlapping hyperspheres and overlapping oriented hypercubes. Can show that this probability vanishes as d becomes large, implying not only that trimers become more ramified or "branch-like" but all larger n-mers (e.g., tetramers, etc.) when $n \ll d$.
- For overlapping hyperspheres,

$$C_3 = -\frac{3 \cdot 2^{d-1} v_2^{int}(D;D)}{v_1(D/2)}. \tag{17}$$

For large d, the leading-order asymptotic result is given by

$$\frac{|C_3|}{C_2^2} \sim \left(\frac{27}{2\pi d}\right)^{1/2} \left(\frac{3}{4}\right)^{d/2}. \tag{18}$$

- For overlapping oriented hypercubes,

$$\frac{|C_3|}{C_2^2} = \left(\frac{3}{4}\right)^{d} \tag{19}$$

Table 1: Trimer Statistics for Overlapping Hyperspheres and Oriented Hypercubes

d	$\lvert C_3\rvert/C_2^2\ _{sphere}$	$\lvert C_3\rvert/C_2^2\ _{cube}$
1	$\frac{3}{4} = 0.7500000000\ldots$	$\left(\frac{3}{4}\right) = 0.7500000000\ldots$
2	$1 - \frac{3\sqrt{3}}{4\pi} = 0.5865033288\ldots$	$\left(\frac{3}{4}\right)^2 = 0.5625000000\ldots$
3	$\frac{15}{32} = 0.4687500000\ldots$	$\left(\frac{3}{4}\right)^3 = 0.4218750000\ldots$
4	$1 - \frac{9\sqrt{3}}{9\pi} = 0.3797549926\ldots$	$\left(\frac{3}{4}\right)^4 = 0.3164062500\ldots$
5	$\frac{159}{512} = 0.3105468750\ldots$	$\left(\frac{3}{4}\right)^5 = 0.2373046875\ldots$
6	$1 - \frac{27\sqrt{3}}{20\pi} = 0.2557059910\ldots$	$\left(\frac{3}{4}\right)^6 = 0.1779785156\ldots$
7	$\frac{867}{4096} = 0.2116699219\ldots$	$\left(\frac{3}{4}\right)^7 = 0.1334838867\ldots$
8	$1 - \frac{837\sqrt{3}}{560\pi} = 0.1759602045\ldots$	$\left(\frac{3}{4}\right)^8 = 0.1001129150\ldots$
9	$\frac{19239}{131072} = 0.1467819214\ldots$	$\left(\frac{3}{4}\right)^9 = 0.07508468628\ldots$
10	$1 - \frac{891\sqrt{3}}{560\pi} = 0.1227963465\ldots$	$\left(\frac{3}{4}\right)^{10} = 0.05631351471\ldots$
11	$\frac{107985}{1048576} = 0.1029825211\ldots$	$\left(\frac{3}{4}\right)^{11} = 0.04223513603\ldots$

Table 2: Tetramer Statistics for Overlapping Hyperspheres and Oriented Hypercubes

d	C_4/C_2^3 sphere	C_4/C_2^3 cube
1	0.5416666667	$\frac{13}{24} = 0.5416666667$
2	0.311070376	$\frac{79}{288} = 0.2743055556$
3	0.1823550119	$\frac{433}{3456} = 0.1252893519$
4	0.1070948900	$\frac{1927}{41472} = 0.04646508488$
5	0.06210757652	$\frac{3793}{497664} = 0.007621608153$
6	0.0349893970	$-\frac{56201}{5971968} = -0.009410800594$
7	0.01866770530	$-\frac{1086527}{71663616} = -0.01516148725$
8	0.008950017	$-\frac{13337273}{859963392} = -0.01550911716$
9	0.003289929140	$-\frac{3403\ 3327}{10319560704} = -0.01359876947$
10	0.000117541	$-\frac{1364831081}{123834728448} = -0.01102139196$
11	−0.001543006376	$-\frac{12654110687}{1048576} = -0.006371786923$

Exact High-d Asymptotics for Percolation Behavior

- **Clearly, threshold η_c for either overlapping hyperspheres or hypercubes must tend to zero as d tends to infinity.**
- **Show that in sufficiently high dimensions, the threshold η_c has the following exact asymptotic expansion:**

$$\eta_c = \frac{1}{2^d} - \frac{C_3}{2^{3d}} - \frac{C_4}{2^{4d}} + O\left(\frac{C_3^2}{2^{5d}}\right), \quad d \gg 1. \tag{20}$$

- **Thus, the corresponding asymptotic expansion for mean number of overlaps per particle is given by**

$$N_c = 1 - \frac{C_3}{2^{2d}} - \frac{C_4}{2^{3d}} + O\left(\frac{C_3^2}{2^{4d}}\right), \quad d \gg 1. \tag{21}$$

- **Hence, in the infinite-dimensional limit, we exactly have**

$$\eta_c \sim \frac{1}{2^d}, \qquad d \to \infty \tag{22}$$

and

$$N_c \sim 1, \qquad d \to \infty, \tag{23}$$

Duality Relation

- First, recall the Ornstein-Zernike (OZ) relation for a general one-component many-particle (not necessarily hard-particle) equilibrium system at number density ρ:

$$h(r) = c(r) + \rho c(r) \otimes h(r) \qquad [P(r) = C(r) + \rho C(r) \otimes P(r)]$$

where $h(r) = g_2(r) - 1$ is total pair correlation function and $c(r)$ is direct correlation function.

- The "compressibility relation" for general equilibrium systems in at number density ρ:

$$\rho k_B T \kappa_T = 1 + \rho \int_{R^d} h(r) dr \qquad \left(S = 1 + \rho \int_{R^d} P(r) dr \right),$$

where k_B is Boltzmann's constant and $\kappa_T \equiv \frac{1}{\rho} \left(\frac{\partial \rho}{\partial p} \right)_T$ is the isothermal compressibility.

- Pair connectedness function $P(r)$ for overlapping hyperspheres is exactly related to the total correlation function $h(r)$ for equilibrium hard-hypersphere fluid in high dimensions via

$$P(r; \rho) = -h(r; -\rho)$$

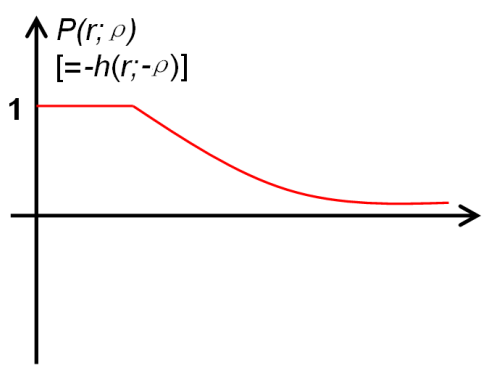

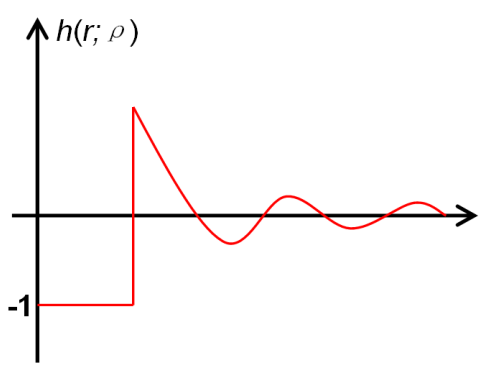

- This duality relation is exact for $d = 1$ and a good approximation for any finite d and $\eta \leq \eta_c$.
- This mapping is exact in the Percus-Yevick approximation for OZ equation.

Decorrelation With Increasing Dimension

- **Decorrelation Principle:**

  1. **Unconstrained pair correlations in disordered many-particle systems that may be present in low dimensions vanish asymptotically in high dimensions;**
  2. **and g_n for any $n \geq 3$ can be inferred entirely (up to some small error) from a knowledge of the number density ρ and the pair correlation function $g_2(\mathrm{r})$.**

Decorrelation With Increasing Dimension

- **Decorrelation Principle:**

  1. **Unconstrained pair correlations in disordered many-particle systems that may be present in low dimensions vanish asymptotically in high dimensions;**
  2. **and g_n for any $n \geq 3$ can be inferred entirely (up to some small error) from a knowledge of the number density ρ and the pair correlation function $g_2(\mathrm{r})$.**

- **Therefore, the freezing-point $g_2(r)$ as $d \to \infty$ tends to the step function. Can show associated packing fraction $\varphi = 1/2^d$.**

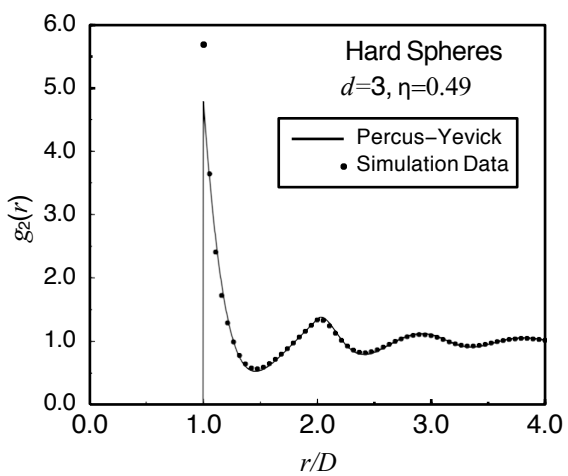

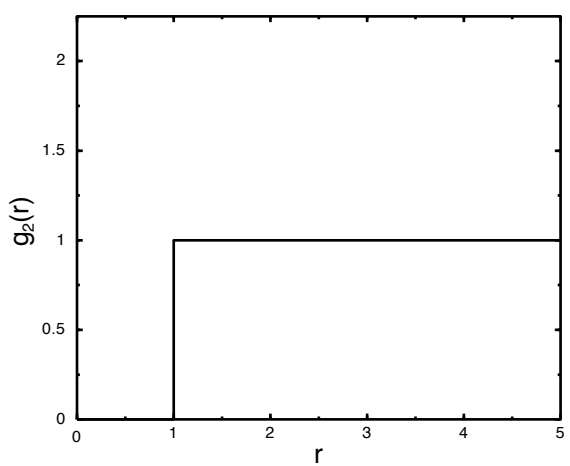

Padé Approximants and Lower Bounds on η_c

- Was empirically observed that $[0, 1]$, $[1, 1]$ and $[2, 1]$ Padé approximants of S provided lower bounds on η_c for $d = 2$ and $d = 3$ (Quintanilla & Torquato, 1996).
- Can prove $[0, 1]$ approximant is a lower bound on η_c and that $[1, 1]$ and $[2, 1]$ approximants are lower bounds η_c for sufficiently small η in any d and for sufficiently large d for $\eta < \eta_0$.
- Easy to show that all $[n, 1]$ Padé approximants are lower bounds on η_c for $d = 1$.
- Consider $[0, 1]$ approximant. Given and Stell (1990) derived the upper bound on $P(r)$:

$$P(r) \leq f(r) + \rho[1 - f(r)][f(r) \otimes P(r)].$$

Note that since $[1 - f(r)] \leq 1$, we also have the weaker upper bound

$$P(r) \leq f(r) + \rho f(r) \otimes P(r). \tag{24}$$

Taking the volume integral of (24) and using the definition (7) for the mean cluster number S yields the following upper bound on the latter:

$$S \leq \frac{1}{1 - S_2 \eta}.$$

Now since this has a pole at $\eta = S_2^{-1}$, implies the following new lower bounds on η_c and N_c:

$$\eta_c \geq \frac{1}{S_2} = \frac{1}{2^d}, \qquad N_c \equiv 2^d \eta_c \geq 1.$$

- These bounds apply to any system of overlapping identical oriented d-dimensional convex particles that possess central symmetry.

Padé Approximants and Lower Bounds on η_c

- [1, 1] Padé approximant of S is given by

$$S \le S_{[1,1]} = \frac{1 + \left(2^d - \frac{S_3}{2^d}\right)\eta}{1 - \frac{S_3}{2^d}\eta}, \qquad \text{for} \quad 0 \le \eta \le \eta_0^{(1)}, \tag{25}$$

provides the following lower bound on η_c for all d:

$$\eta_c \ge \eta_0^{(1)} = \frac{1}{2^d\left(1 + \frac{C_3}{2^{2d}}\right)}. \tag{26}$$

- [2, 1] Padé approximant of S is given by

$$S \le S_{[1,1]} = \frac{1 + \left(2^d - \frac{S_4}{S_3}\right)\eta + \left(S_3 - \frac{2^d S_4}{S_3}\right)\eta^2}{1 - \frac{S_4}{S_3}\eta}, \qquad \text{for} \quad 0 \le \eta \le \eta_0^{(2)}, \tag{27}$$

provides the following lower bound on η_c for all d:

$$\eta_c \ge \eta_0^{(2)} = \frac{1 + \frac{C_3}{2^{2d}}}{2^d\left(1 + \frac{2C_3}{2^{2d}} + \frac{C_4}{2^{3d}}\right)}. \tag{28}$$

This becomes asymptotically exact in high d, and provides a very good estimate of η_c, even in low dimensions!

Table 3: Results for Overlapping Hyperspheres. Simulation data due to Krüger (2003)

d	η_c^{PU}	η_c	η_c^L from [2, 1]	η_c^L from [1, 1]	η_c^L from [0, 1
2		**1.1282**	0.7487424583 . . .	0.604599 . . .	0.250000 . .
3	0.500000 . . .	**0.3418**	0.2712064151 . . .	0.235294 . . .	0.125000 . .
4	0.138093 . . .	**0.1300**	0.1115276079 . . .	0.100766 . . .	0.0625000 . .
5	0.0546701 . . .	**0.0543**	0.04885427359 . . .	0.0453257 . . .	0.0312500 . .
6	0.0236116 . . .	**0.02346**	0.02221179439 . . .	0.0209930 . . .	0.0156250 . .
7	0.0106853 . . .	**0.0105**	0.01034527214 . . .	0.00991018 . . .	0.00781250 .
8	0.00497795 . . .	**0.00481**	0.004899178686 . . .	0.00474036 . . .	0.00390625 .
9	0.00236383 . . .	**0.00227**	0.002348006636 . . .	0.00228912 . . .	0.00195312 .
10	0.00113725 . . .	**0.00106**	0.001135342587 . . .	0.00111326 . . .	0.000976562 .
11	0.000552172 . . .	**0.000505**	0.0005526829831 . . .	0.000544338 . . .	0.000488281 .

- **Simulation data begins to violate best lower bound at** $d = 8$
- **Wagner, Balberg & Klein (2006) incorrectly found that** $N_c = 2^d \eta_c$ **is a nonmonotonic function of** d **and incorrectly concluded that hyperspheres have lower thresholds than hypercubes in higher dimensions** ($d \geq 8$).
- **These numerical threshold estimates were refined in a follow-up article: Torquato & Jiao, J. Chem. Phys. (2012).**

Overlapping Hyperspheres and Oriented Hypercubes

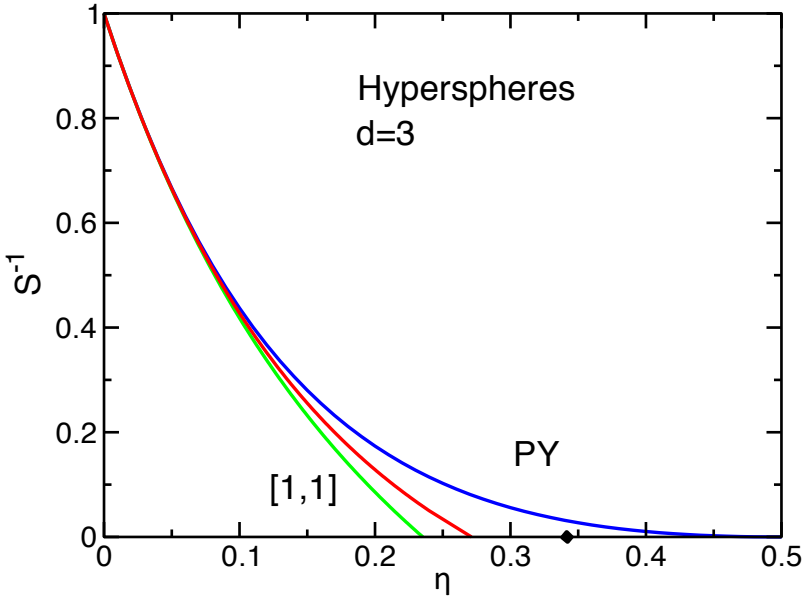

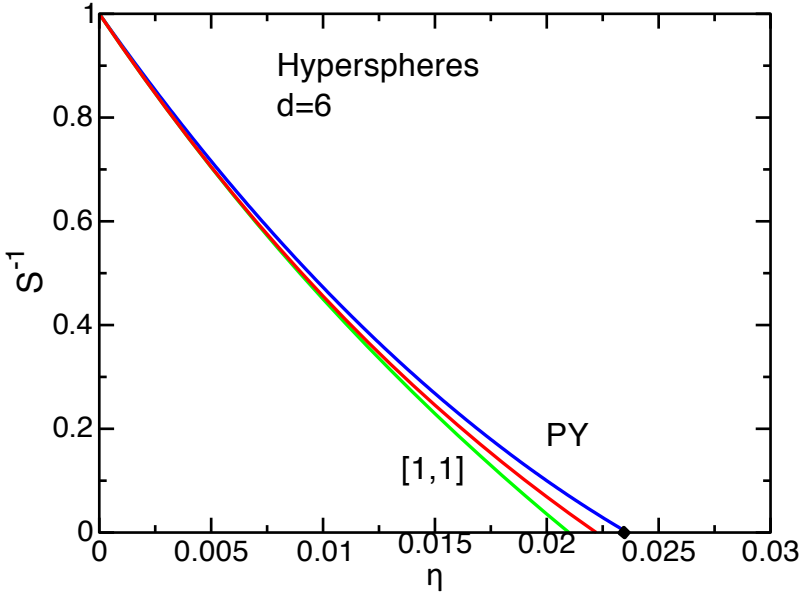

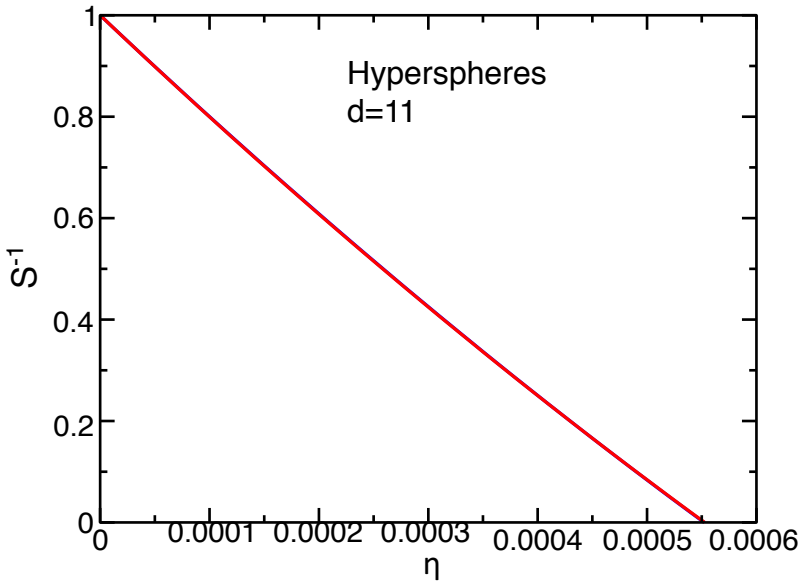

- **Qualitatively simialr results were obtained for hypercubes.**

Extension to d-dimensional Hyperparticles of General Convex Shap

- **For overlapping hyperparticles of general anisotropic shape of volume v_1 with specified orientational PDF $p(\omega)$ in d dimensions, the simplest lower bounds on η_c and N_c generalize as follows:**

$$\eta_c \geq \frac{v_1}{v_{\mathbf{ex}}}, \qquad (29)$$

$$N_c \equiv \eta_c \frac{v_{\mathbf{ex}}}{v_1} \geq 1,$$

where

$$v_{\mathbf{ex}} = \int_{R^d} f(r, \omega) p(\omega) dr d\omega.$$

- **Exclusion volumes are known for some convex nonspherical shapes that are randomly oriented in two and three dimensions (Onsager 1948; Kihara 1953; Boublik 1975).**
- **Evaluated lower bound for a variety of randomly oriented nonspherical particles in two and three dimensions.**
- **Showed that the lower bound is relatively tight and improves in accuracy in any fixed d as the particle shape becomes more anisotropic.**

Effect of Dimensionality on η_c for Nonspherical Hyperparticles

Torquato and Jiao, Phys. Rev. E, 2013

Exclusion-Volume Formula in $\mathbb{R}^d$

- **Have derived a general formula for $v_{\mathbf{ex}}$ for randomly oriented convex hyperparticle in any d:**

$$v_{\mathbf{ex}} = 2v_1 + \frac{2(2^{d-1} - 1)}{d} s_1 \bar{R},$$

where s_1 is the d-dimensional surface area of the particle and $\bar{R}$ is its radius of mean curvature. Recovers well-known special cases for $d = 2$ and $d = 3$.

Effect of Dimensionality on η_c for Nonspherical Hyperparticles

Torquato and Jiao, Phys. Rev. E, 2013

Exclusion-Volume Formula in $\mathbb{R}^d$

- Have derived a general formula for $v_{\mathbf{ex}}$ for randomly oriented convex hyperparticle in any d:

$$v_{\mathbf{ex}} = 2v_1 + \frac{2(2^{d-1} - 1)}{d} s_1 \bar{R},$$

where s_1 is the d-dimensional surface area of the particle and $\bar{R}$ is its radius of mean curvature. Recovers well-known special cases for $d = 2$ and $d = 3$.

An Isoperimetric Inequality

Theorem: Among all convex hyperparticles of nonzero volume, the hypersphere possesses the smallest scaled exclusion volume $v_{ex}/v_1 = 2^d$.

- This theorem together with exclusion-volume formula leads to the following inequality involving s_1, $\bar{R}$ and v_1:

$$s_1 \bar{R} \geq d v_1, \tag{30}$$

where the equality holds for hyperspheres only. This is a special type of isoperimetric inequality.

Radius of Mean Curvature (Mean Width)

- Consider any convex body K in d-dimensional Euclidean space R^d to be trapped entirely between two impenetrable parallel $(d-1)$-dimensional hyperplanes that are orthogonal to a unit vector n in R^d. The "width" of a body $w(\mathrm{n})$ in the direction n is the distance between the closest pair of such parallel hyperplanes.
- The mean width $\bar{w}$ is the average of the width $w(\mathrm{n})$ such that n is uniformly distributed over the unit sphere $S^{d-1} \in \mathrm{R}^d$.

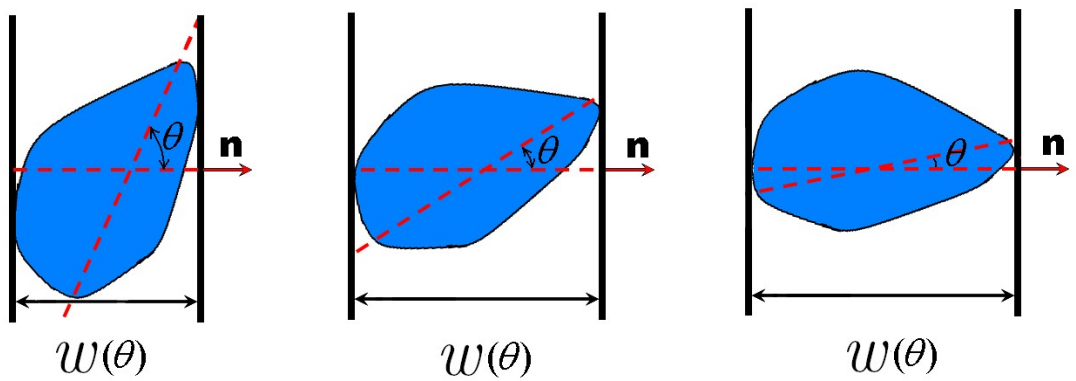

- The radius of mean curvature $\bar{R}$ of a convex body is trivially related to its mean width $\bar{w}$ via

$$\bar{R} = \frac{\bar{w}}{2} \tag{31}$$

Steiner Formula

- **The famous Steiner formula expresses the volume v_ϱ of the parallel body in $\mathbb{R}^d$ at distance ϱ as a polynomial in ϱ and in terms of geometrical characteristics of the convex body K, i.e.,**

$$v_\varrho = \sum_{k=0}^{d} W_k \varrho^k, \tag{32}$$

where W_k are trivially related to the quermassintegrals or Minkowski functionals. Of particular interest is the lineal characteristic, i.e., the $(d-1)$th coefficient:

$$W_{d-1} = \Omega(d)\bar{R}, \tag{33}$$

where $\bar{R}$ is the radius of mean curvature and

$$\Omega(d) = \frac{d\pi^{d/2}}{\Gamma(1+d/2)} \tag{34}$$

is the total solid angle contained in d-dimensional sphere.

Steiner Formula

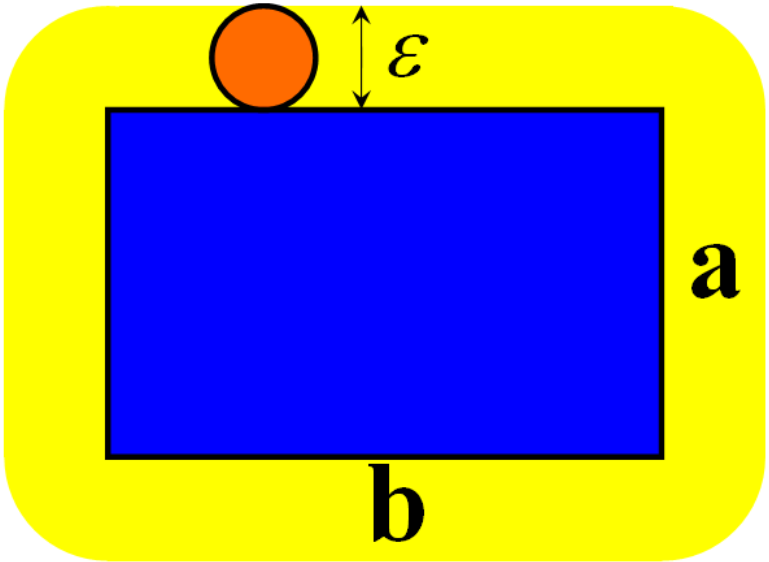

Figure 1: Parallel body for a rectangle.

- **For a 3-cube of side length a, the volume of the parallel body**

$$v_\varrho = v_1 + s_1\varrho + 3a\pi\varrho^2 + \frac{4\pi}{3}\varrho^3$$

and hence radius of mean curvature is

$$\bar{R} = \frac{3}{4}a$$

Analytical Expressions for Exclusion Volumes in R^d

- **We have analytically derived formulas for the exclusion volumes for a variety of nonspherical convex bodies in 2, 3 and arbitrary dimensions d.**
  - **Platonic solids, spherocylinders, and parallelpipeds in R^3**
  - **d-cube (hypercube)**
  - **r. ectangular parallelpiped (hyperrectangular parallelpiped)**
  - **s. pherocylinder (hyperspherocylinder)**
  - **regular d-crosspolytope (hyperoctahedron or orthoplex)**
  - **A regular d-simplex (hypertetrahedron)**

- **Note that the hypercube, hyperoctahedron and hypertetrahedron are the only regular polytopes for $d \geq 5$.**

Exclusion Volume for Platonic Solids

Table 4: **The numerical values of the dimensionless exclusion volumes v_{ex}/v_1 of 3D regular polyhedra and sphere.**

K	v_{ex}/v_1
Tetrahedron	$\frac{3}{4\pi}\cos^{-1}(-\frac{1}{3}) = 15.40743\ldots$
Cube	**11**
Octahedron	$\frac{3}{2\pi}\cos^{-1}(\frac{1}{3}) = 10.63797\ldots$
Dodecahedron	$\frac{30}{8\pi}\cos^{-1}(\frac{1}{\sqrt{5}}) = 9.12101\ldots$
Icosahedron	$\frac{30}{8\pi}\cos^{-1}(\frac{\sqrt{5}}{3}) = 8.91526\ldots$
Sphere	**8**

Exclusion Volume for Regular Polytopes in R^d

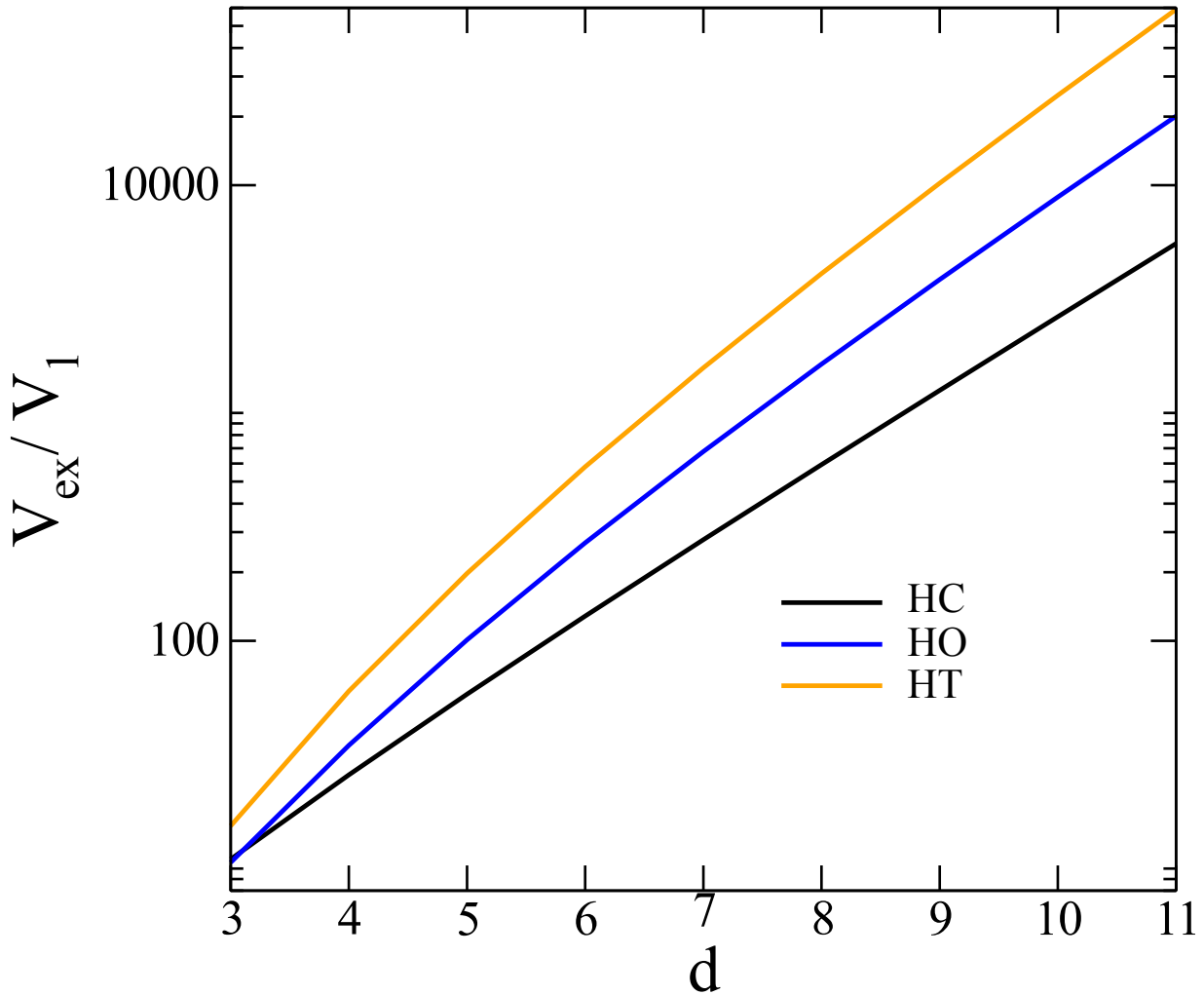

Figure 2: The dimensionless exclusion volume v_{ex}/v_1 versus dimension d for the three convex regular polytopes: hypercube, hyperoctahedron and hypertetrahedron.

Conjecture for Maximum-Threshold Convex Body

- **Recall that the dimensionless exclusion volume $v_{\mathbf{ex}}/v_1$, among all convex bodies in R^d with a nonzero d-dimensional volume, is minimized for hyperspheres. Also, threshold η_c of a d-dimensional hypersphere exactly tends to $v_1/v_{\mathbf{ex}} = 2^{-d}$ in the high-dimensional limit.**

- **These properties together with the principle that low-d percolation properties encode high-d information, leads us to the following conjecture:**
  Conjecture: The percolation threshold η_c among all systems of overlapping randomly oriented convex hyperparticles in R^d having nonzero volume is maximized by that for hyperspheres, i.e.,

$$(\eta_c)_S \geq \eta_c, \tag{35}$$

  where $(\eta_c)_S$ is the threshold of overlapping hyperspheres.

- **Similar reasoning also suggests that the dimensionless exclusion volume $v_{\mathbf{ex}}/v_{\mathbf{eff}}$ associated with a convex $(d-1)$-dimensional hyperplate in R^d is minimized by the $(d-1)$-dimensional hypersphere, which consequently would have the highest percolation threshold among all convex hyperplates.**

Accurate Scaling Relation for η_c for Nonspherical Convex Hyperpartic

- Guided by the high-dimensional behavior of η_c, the aforementioned conjecture for hyperspheres and the functional form of the lower bound $\eta_c \geq v_1/v_{\mathbf{ex}}$, we propose the following scaling relation for the threshold η_c of overlapping nonspherical convex hyperparticles of arbitrary shape and orientational distribution that possess nonzero volumes for any dimension d:

$$\eta_c \approx \left(\frac{v_{\mathbf{ex}}}{v_1}\right)_S \left(\frac{v_1}{v_{\mathbf{ex}}}\right) (\eta_c)_S = 2^d \left(\frac{v_1}{v_{\mathbf{ex}}}\right) (\eta_c)_S, \tag{36}$$

where $(\eta_c)_S$ is the threshold for a hypersphere system.

- The scaling relation (36) is also an upper bound on η_c, i.e.,

$$\eta_c \geq 2^d \left(\frac{v_1}{v_{\mathbf{ex}}}\right) (\eta_c)_S. \tag{37}$$

- For a zero-volume convex $(d-1)$-dimensional hyperplate in R^d, reference system is $(d-1)$-dimensional hypersphere of characteristic radius r with effective volume $v_{\mathbf{eff}}$, yielding the scaling relation

$$\eta_c \approx 2^d \left(\frac{v_{\mathbf{eff}}}{v_{\mathbf{ex}}}\right) (\eta_c)_{SHP}, \tag{38}$$

where $(\eta_c)_{SHP}$ is the threshold for a $(d-1)$-dimensional hypersphere.

Scaling Relation: Three Dimensions

Table 5: Percolation threshold η_c of certain overlapping convex particles K with random orientations in R^3 predicted from scaling relation and the associated threshold values η^*_c for regular polyhedra (obtained from our numerical simulations) and spheroids.

K	η_c^*	η_c
Sphere	0.3418	
Tetrahedron	0.1701	0.1774
Icosahedron	0.3030	0.3079
Decahedron	0.2949	0.2998
Octahedron	0.2514	0.2578
Cube	0.2443	0.2485
Oblate spheroid $a = c = 100b$	0.01255	0.01154
Oblate spheroid $a = c = 10b$	0.1118	0.104
Oblate spheroid $a = c = 2b$	0.3050	0.3022
Prolate spheroid $a = c = b/2$	0.3035	0.3022
Prolate spheroid $a = c = b/10$	0.09105	0.104
Prolate spheroid $a = c = b/100$	0.006973	0.01154
Parallelpiped $a_2 = a_3 = 2a_1$		0.2278
Cylinder $h = 2a$		0.4669
Spheroclyinder $h = 2a$		0.2972

Scaling Relation: Plates in R^3

Table 6: Percolation threshold η_c of certain overlapping convex plates K with random orientations in R^3 predicted from scaling relation.

K	η_c^*	η_c
Circular disk	0.9614	
Square plate	0.8647	0.8520
Triangular plate	0.7295	0.7475
Elliptical plate $b = 3a$	0.735	0.7469
Rectangular plate $a_2 = 2a_1$		1.0987

Scaling Relation: Hyperparticle in Dimensions Four Through Eleve

Table 7: **Percolation threshold η_c of certain d-dimensional randomly overlapping hyperparticles predicted from the scaling relqtion for $4 \leq d \leq 11$, including hypercubes (HC), hyperrectangular parallelpiped (HRP) of aspect ratio 2 (i.e., $a_1 = 2a$ and $a_i = a$ for $i = 2, \ldots, d$), hyperspherocylinder (HSC) of aspect ratio 2 (i.e., $h = 2a$), hyperoctahedra (HO) and hypertetrahedra (HT).**

Dimension	HC	HRP	HSC	HO	
$d = 4$	8.097×10^{-2}	7.452×10^{-2}	1.109×10^{-1}	6.009×10^{-2}	3.47
$d = 5$	2.990×10^{-2}	2.775×10^{-2}	4.599×10^{-2}	1.724×10^{-2}	8.80
$d = 6$	1.167×10^{-2}	1.092×10^{-2}	1.975×10^{-2}	5.560×10^{-3}	2.58
$d = 7$	4.846×10^{-3}	4.568×10^{-3}	8.899×10^{-3}	1.986×10^{-3}	8.51
$d = 8$	2.116×10^{-3}	2.006×10^{-3}	4.167×10^{-3}	7.659×10^{-4}	3.07
$d = 9$	9.584×10^{-4}	9.133×10^{-4}	2.007×10^{-3}	3.129×10^{-4}	1.18
$d = 10$	4.404×10^{-4}	4.214×10^{-4}	9.746×10^{-4}	1.314×10^{-4}	4.69
$d = 11$	2.044×10^{-4}	1.963×10^{-4}	4.754×10^{-4}	5.632×10^{-5}	1.91

Scaling Relation: Hyperparticles in Dimensions 4 Through 11

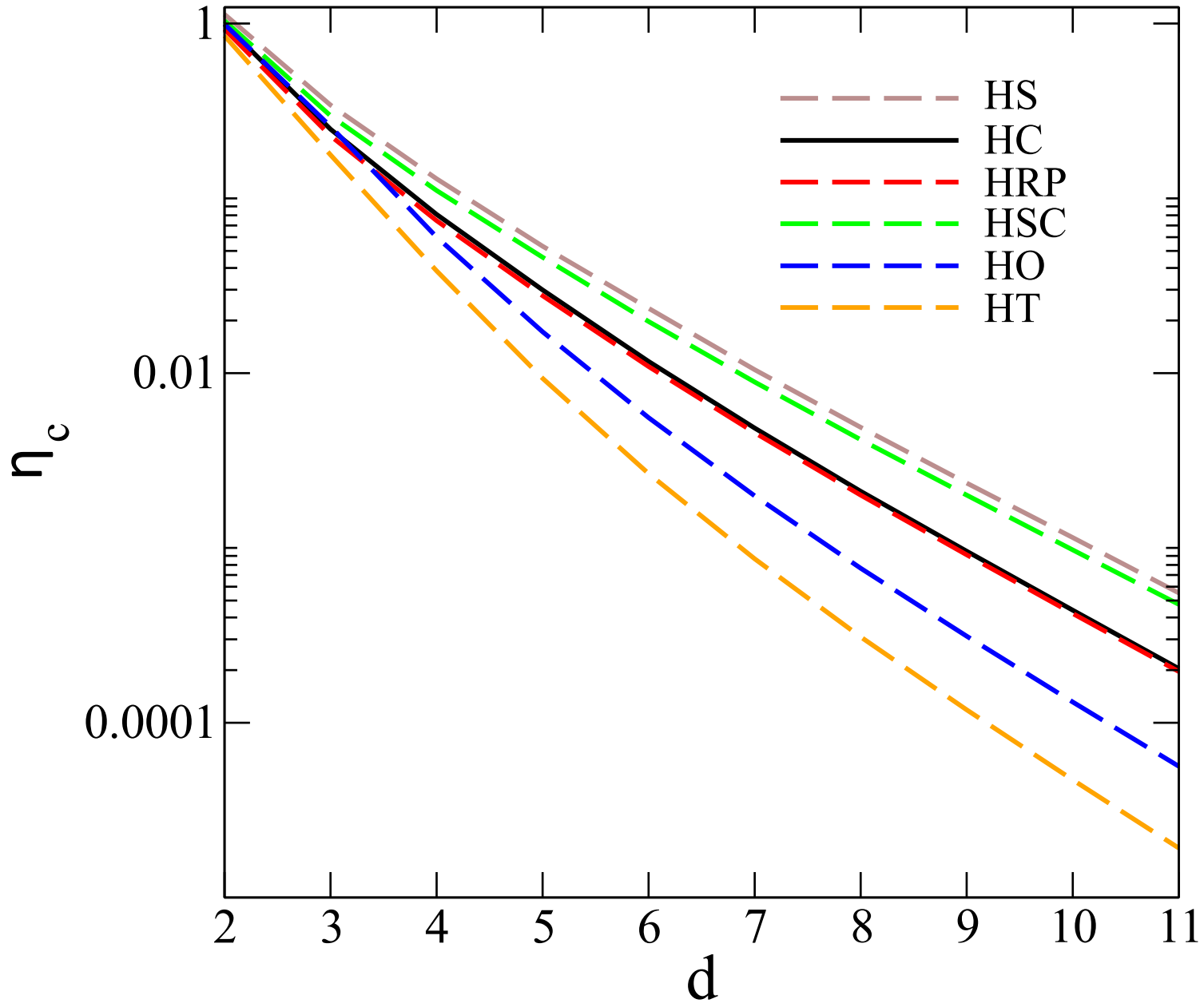

Scaling Relation: Hyperplates for Dimensions 4 Through 11

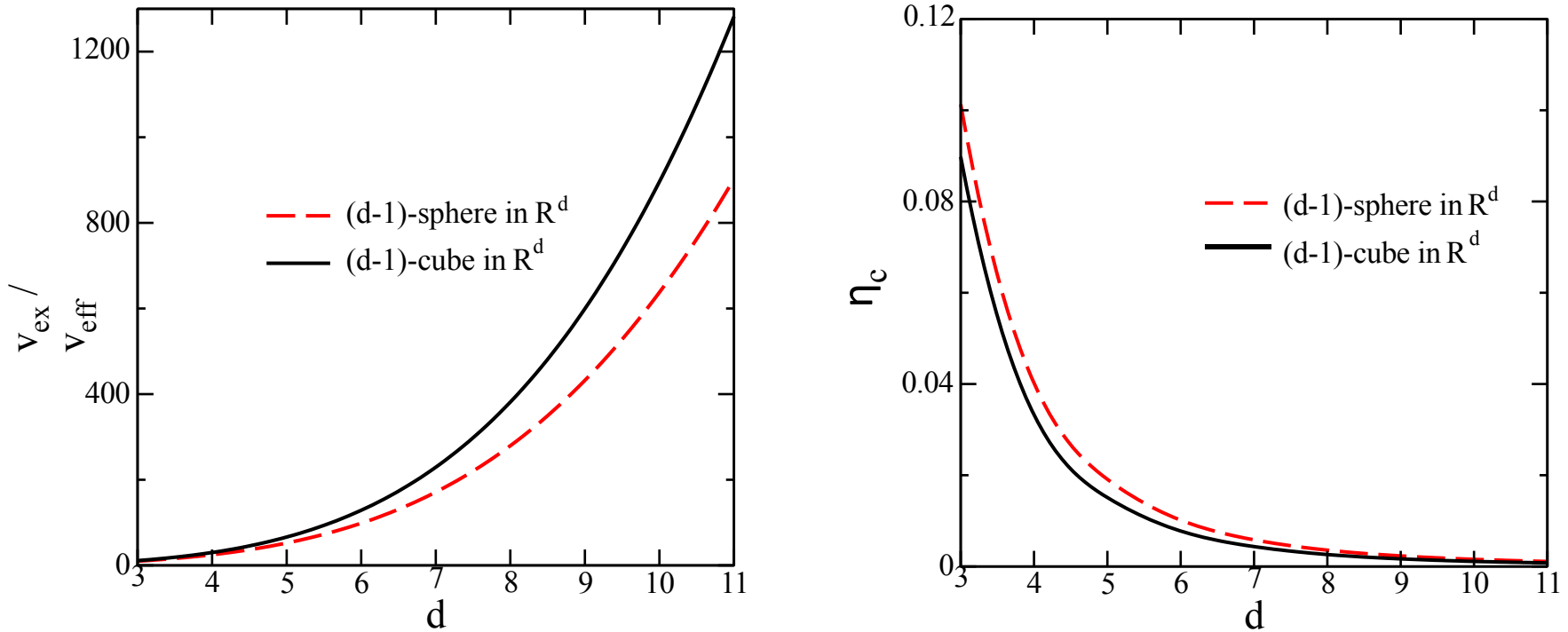

Figure 4: Left panel: Dimensionless exclusion volume v_{ex}/v_{eff} versus dimension d for spherical and cubical hyperplates. Right panel: Lower bounds on the percolation threshold η_c versus dimension d for spherical and cubical hyperplates.

Conclusions

- A systematic and predictive theory for continuum percolation models of hyperspheres and nonspherical hyperparticles across all Euclean space dimensions has been obtained.
- Analysis was aided by a remarkable duality between the equilibrium hard-hypersphere (hypercube) fluid system and the continuum percolation model of overlapping hyperspheres (hypercubes).
- Low-dimensional results encode high-dimensional information.
- Analytical estimates have been used to assess previous simulation results for η_c up to twenty dimensions.

Extensions to Lattice Percolation in High Dimensions

- Showed that analogous lower-order Padé approximants lead also to bounds on the percolation threshold for lattice-percolation models (e.g., site and bond percolation) in arbitrary dimension.

Torquato and Jiao, Phys. Rev. E, 2013

Disordered Hyperuniform Materials: New States of Amorphous Matter

Salvatore Torquato

Department of Chemistry,

Department of Physics,

Princeton Institute for the Science and Technology of Materials,

and Program in Applied & Computational Mathematics

Princeton University

States (Phases) of Matter

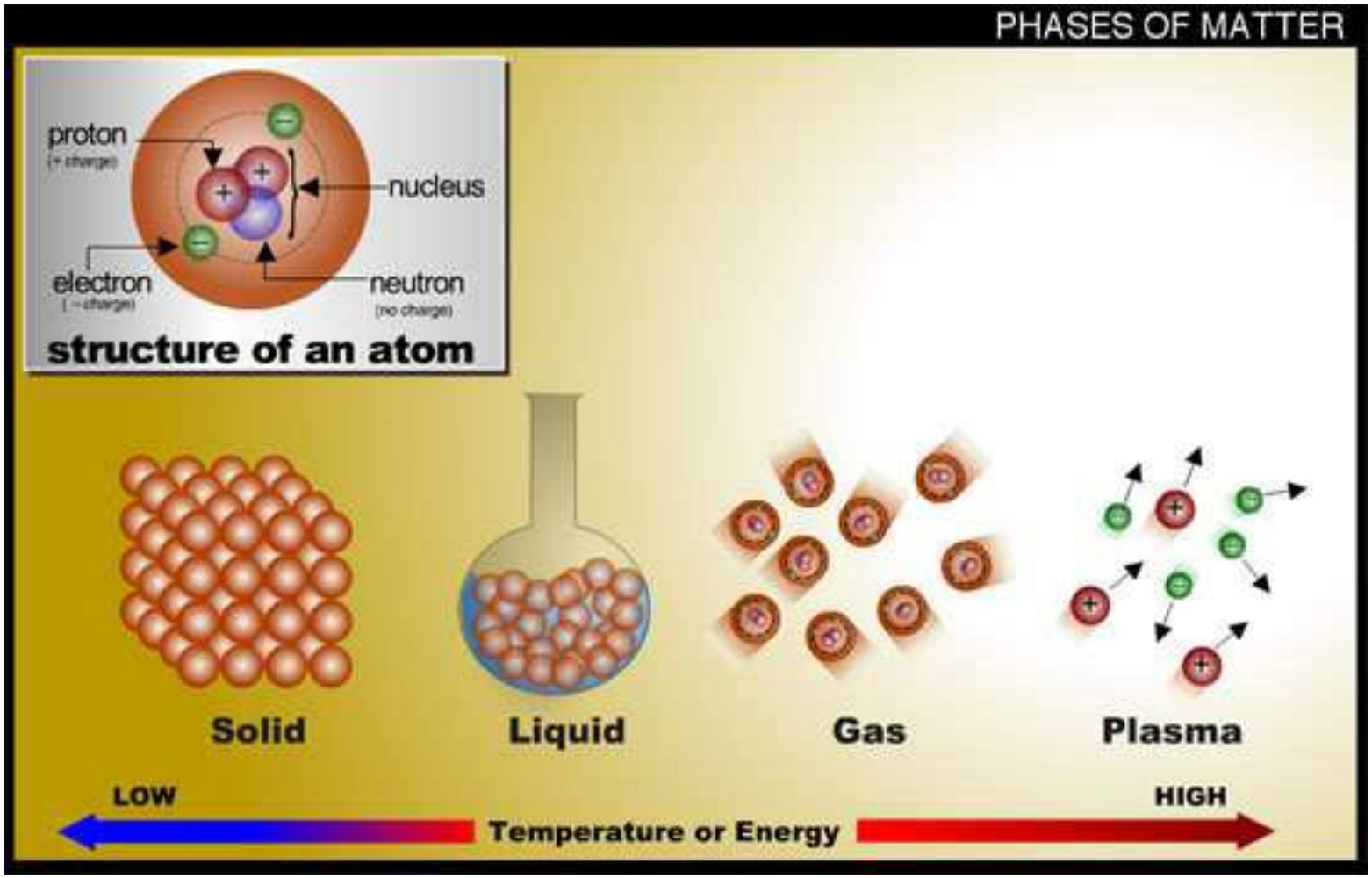

States (Phases) of Matter

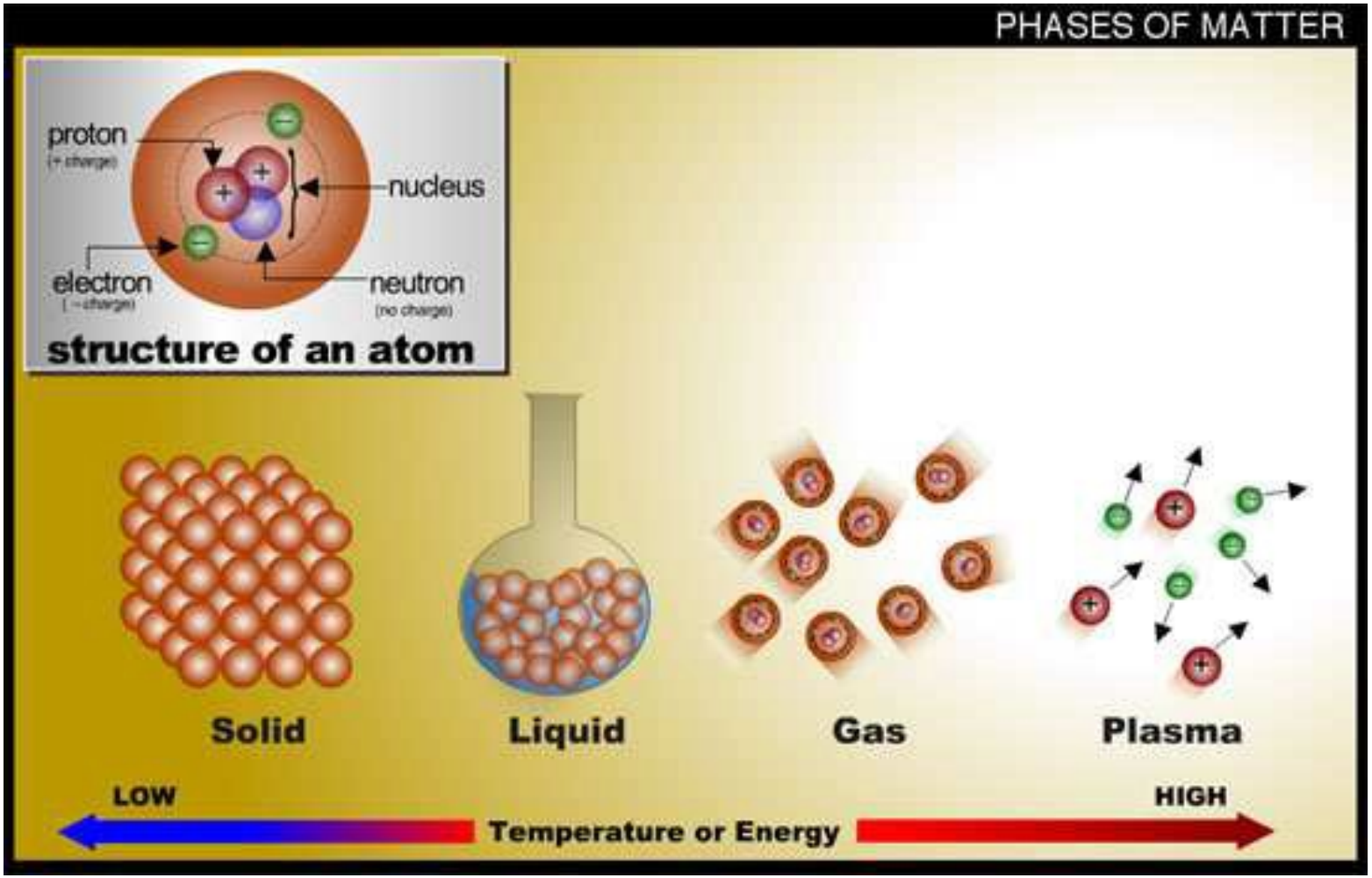

- We now know there are a multitude of distinguishable states of matter, e.g., quasicrystals and liquid crystals, which break the continuous translational and rotational symmetries of a liquid differently from a solid crystal.

HYPERUNIFORMITY

- A hyperuniform many-particle system is one in which normalized density fluctuations are completely suppressed at very large lengths scales.

HYPERUNIFORMITY

- A hyperuniform many-particle system is one in which normalized density fluctuations are completely suppressed at very large lengths scales.

- Disordered hyperuniform many-particle systems can be regarded to be new ideal states of disordered matter in that they

  (i)behave more like crystals or quasicrystals in the manner in which they suppress large-scale density fluctuations, and yet are also like liquids and glasses since they are statistically isotropic structures with no Bragg peaks;

  (ii) can exist as both as equilibrium and nonequilibrium phases;

  (iii) come in quantum-mechanical and classical varieties;

(iv) and, appear to be endowed with unique bulk physical properties.

Understanding such states of matter require new theoretical tools.

HYPERUNIFORMITY

- A hyperuniform many-particle system is one in which normalized density fluctuations are completely suppressed at very large lengths scales.

- Disordered hyperuniform many-particle systems can be regarded to be new ideal states of disordered matter in that they

  (i)behave more like crystals or quasicrystals in the manner in which they suppress large-scale density fluctuations, and yet are also like liquids and glasses since they are statistically isotropic structures with no Bragg peaks;

  (ii) can exist as both as equilibrium and nonequilibrium phases;

  (iii) come in quantum-mechanical and classical varieties;

(iv) and, appear to be endowed with unique bulk physical properties.

Understanding such states of matter require new theoretical tools.

- All perfect crystals (periodic systems) and quasicrystals are hyperuniform.

HYPERUNIFORMITY

- A hyperuniform many-particle system is one in which normalized density fluctuations are completely suppressed at very large lengths scales.

- Disordered hyperuniform many-particle systems can be regarded to be new ideal states of disordered matter in that they

  (i)behave more like crystals or quasicrystals in the manner in which they suppress large-scale density fluctuations, and yet are also like liquids and glasses since they are statistically isotropic structures with no Bragg peaks;

  (ii) can exist as both as equilibrium and nonequilibrium phases;

  (iii) come in quantum-mechanical and classical varieties;

(iv) and, appear to be endowed with unique bulk physical properties.

Understanding such states of matter require new theoretical tools.

- All perfect crystals (periodic systems) and quasicrystals are hyperuniform.

- Thus, hyperuniformity provides a unified means of categorizing and characterizing crystals, quasicrystals and such special disordered systems.

Local Density Fluctuations for General Point Patterns

Torquato and Stillinger, PRE (2003)

- **Points can represent molecules of a material, stars in a galaxy, or trees in a forest. Let Ω represent a spherical window of radius R in d-dimensional Euclidean space R^d.**

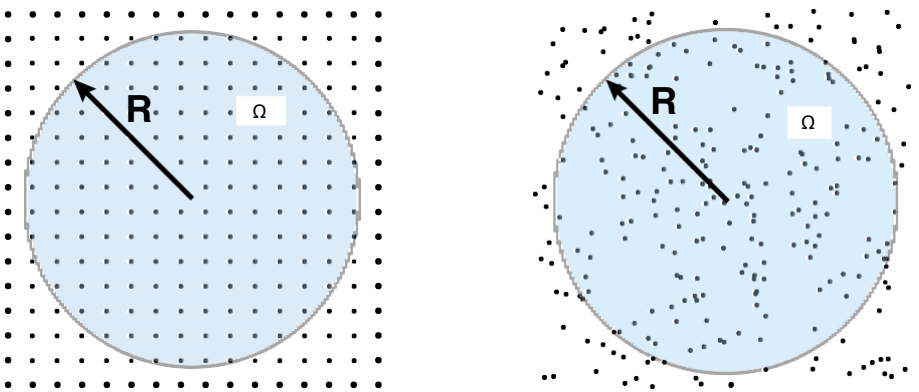

Average number of points in window of volume $v_1(R)$: $\langle N(R)\rangle = \rho v_1(R) \sim R^d$

Local number variance: $\sigma^2(R) \equiv \langle N^2(R)\rangle - \langle N(R)\rangle^2$

Local Density Fluctuations for General Point Patterns

Torquato and Stillinger, PRE (2003)

- **Points can represent molecules of a material, stars in a galaxy, or trees in a forest. Let Ω represent a spherical window of radius R in d-dimensional Euclidean space R^d.**

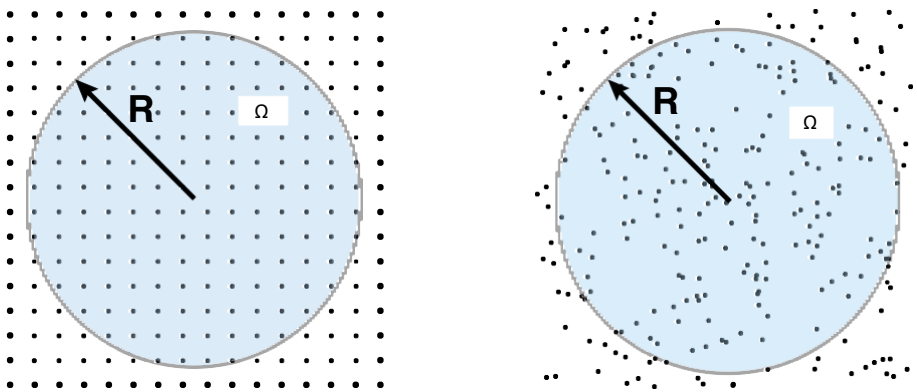

Average number of points in window of volume $v_1(R)$: $(N(R)) = \rho v_1(R) \sim R^d$

Local number variance: $\sigma^2(R) \equiv (N^2(R)) - (N(R))^2$

- **For a Poisson point pattern and many disordered point patterns, $\sigma^2(R) \sim R^d$.**
- **We call point patterns whose variance grows more slowly than R^d (window volume) hyperuniform . This implies that structure factor $S(k) \to 0$ for $k \to 0$.**
- **All perfect crystals and many perfect quasicrystals are hyperuniform such that $\sigma^2(R) \sim R^{d-1}$: number variance grows like window surface area.**

SCATTERING AND DENSITY FLUCTUATIONS

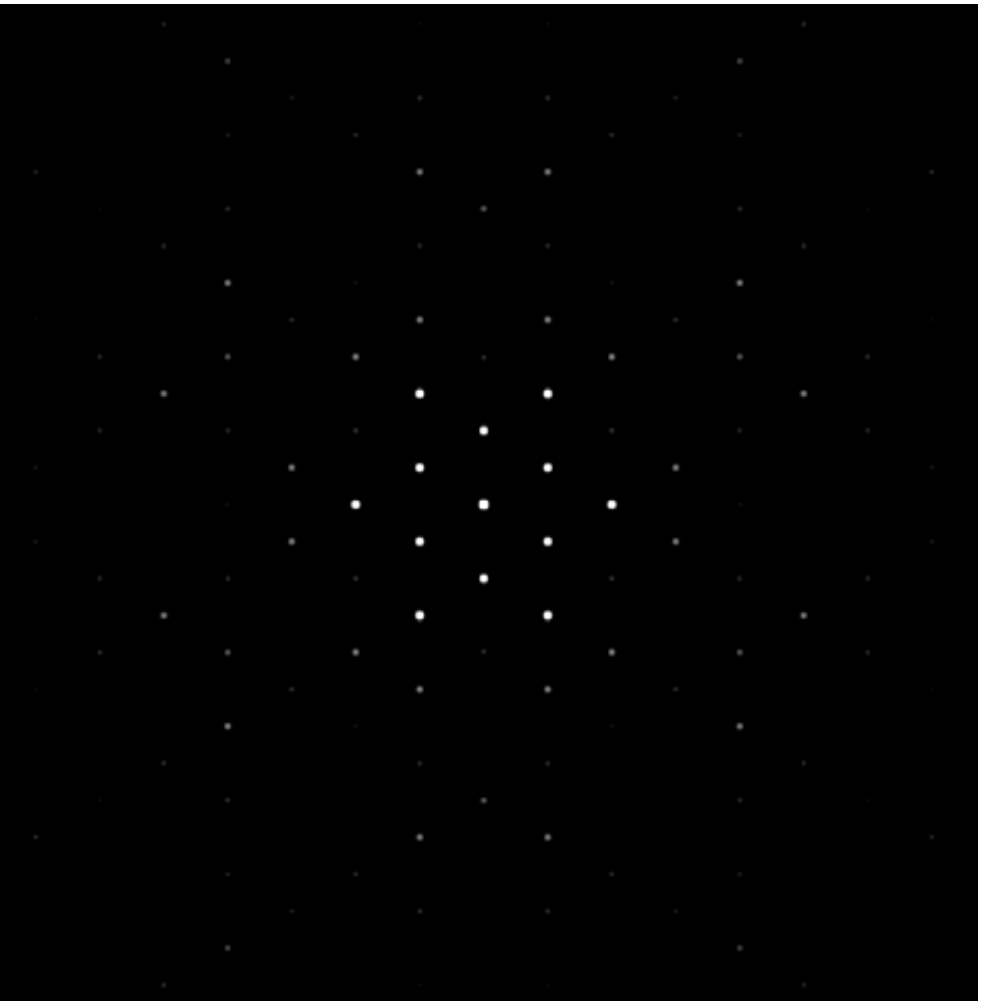

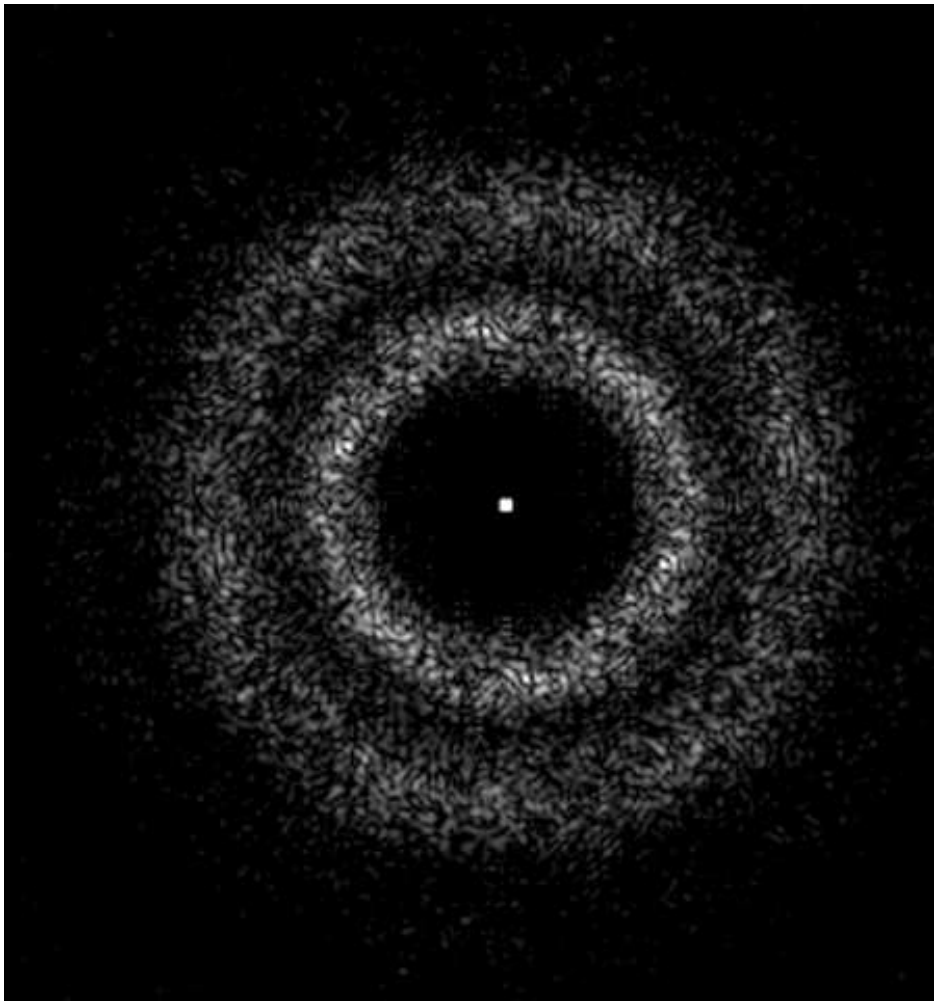

Pair Statistics in Direct and Fourier Spaces

- For particle systems in $\mathbb{R}^d$ at number density ρ , $g_2(r)$ is a nonnegative radial function that is proportional to the probability density of pair distances r.
- The nonnegative structure factor $S(k) \equiv 1 + \rho \tilde{h}(k)$ is obtained from the Fourier transform of $h(r) = g_2(r) - 1$, which we denote by $\tilde{h}(k)$.

Poisson Distribution (Ideal Gas)

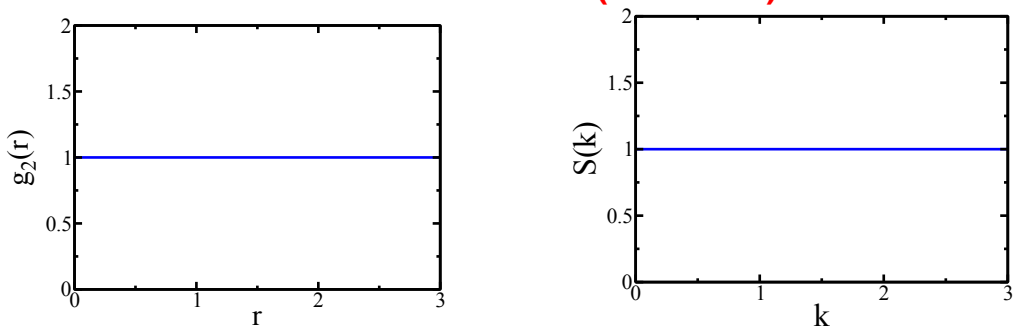

Liquid

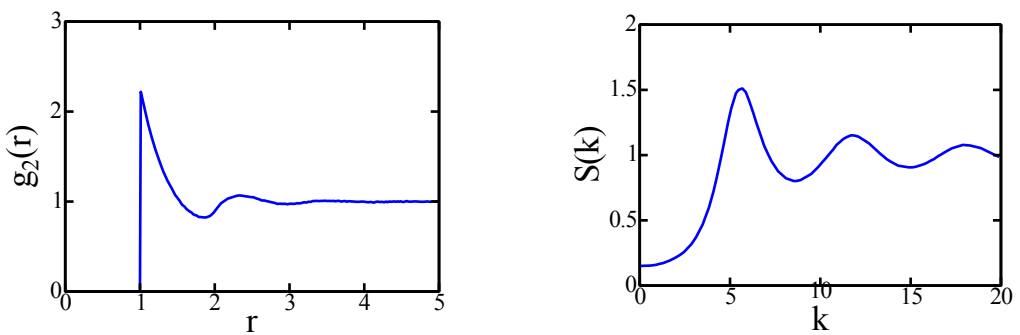

Disordered Hyperuniform System

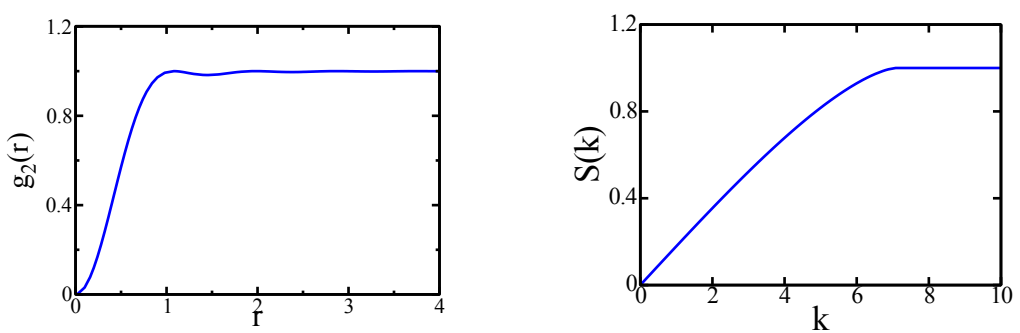

Hidden Order on Large Length Scales

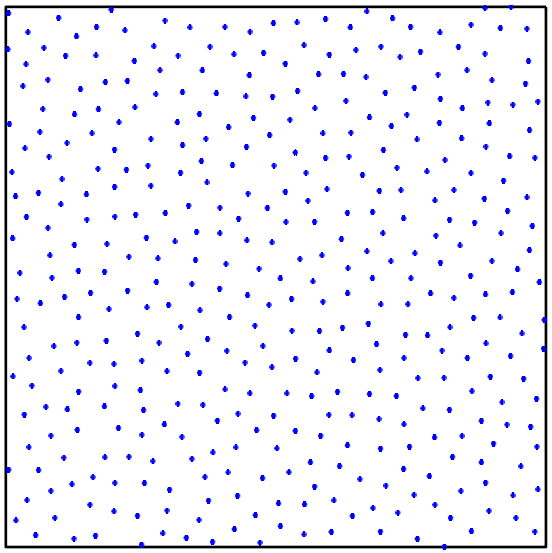

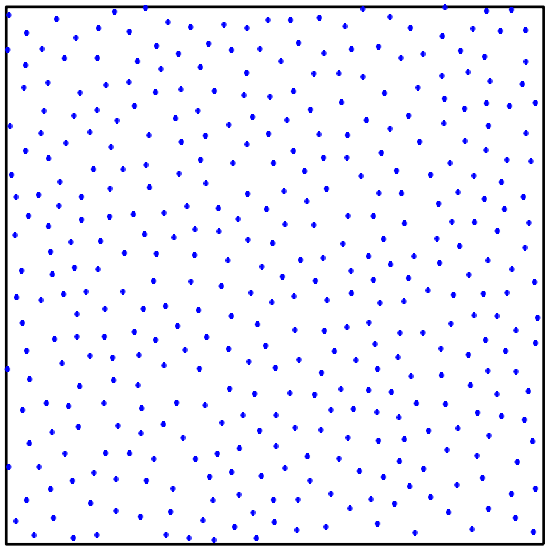

Which is the hyperuniform pattern?

Scaled Number Variance for 3D Systems at Unit Density

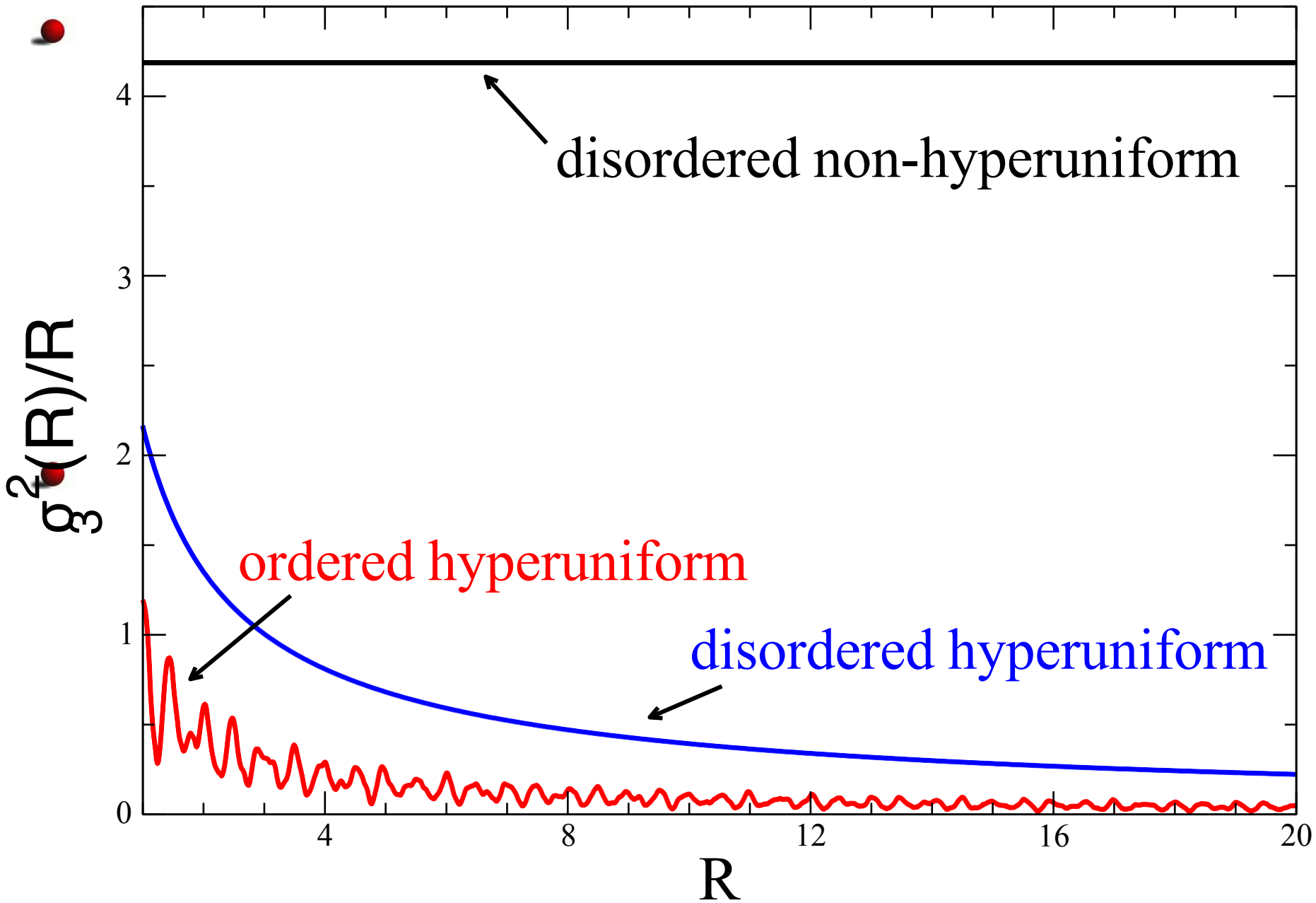

Remarks About Equilibrium Systems

- For single-component systems in equilibrium at average number density ρ, where $(\,)_*$ denotes an average in the grand canonical ensemble.

  Some observations

  $$\rho k_B T \kappa_T = \frac{(N^2)_* - (N)_*^2}{(N)_*} = S(k=0) = 1 + \rho \int_{\mathbb{R}^d} h(r)\,dr$$

  Any ground state ($T = 0$) in which the isothermal compressibility κ_T is bounded and positive must be hyperuniform. This includes crystal ground states as well as exotic disordered ground states, described later.

  However, in order to have a hyperuniform system at positive T, the isothermal compressibility must be zero; i.e., the system must be incompressible.

  Note that generally $\rho k T \kappa_T \neq S(k=0)$.

$$X = \frac{S(k=0)}{\rho k_B T \kappa_T} - 1 : \quad \text{Nonequilibrium index}$$

ENSEMBLE-AVERAGE FORMULATION

- **For a translationally invariant point process at number density ρ in $\mathbb{R}^d$:**

$$\sigma^2(R) = (N(R))\left[1 + \rho \int_{\mathbb{R}^d} h(\mathrm{r})\alpha(\mathrm{r}; R)\, d\mathrm{r}\right]$$

$\alpha(\mathrm{r}; R)$**- scaled intersection volume of 2 windows of radius R separated by r**

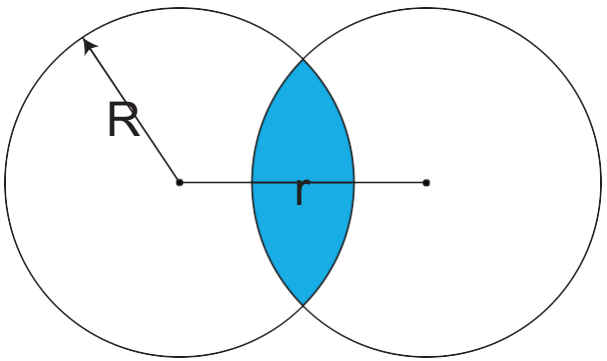

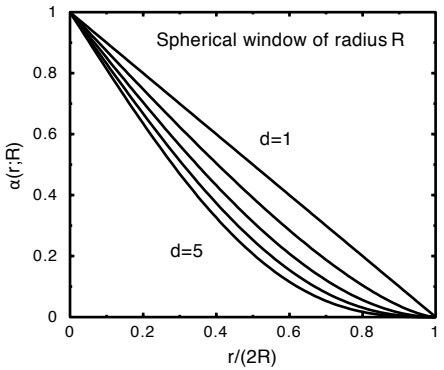

ENSEMBLE-AVERAGE FORMULATION

- For a translationally invariant point process at number density ρ in $\mathbb{R}^d$:

$$\sigma^2(R) = (N(R))\left[1 + \rho \int_{\mathbb{R}^d} h(\mathbf{r})\alpha(\mathbf{r};R)\,d\mathbf{r}\right]$$

$\alpha(\mathbf{r};R)$- scaled intersection volume of 2 windows of radius R separated by $\mathbf{r}$

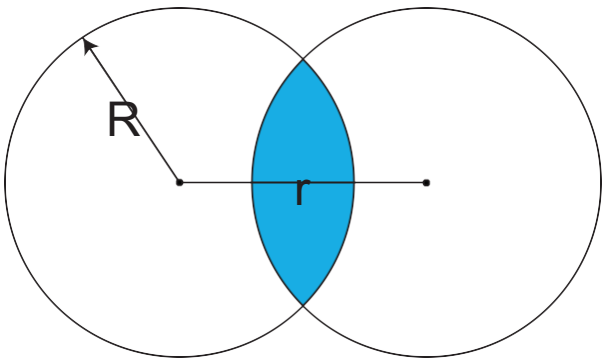

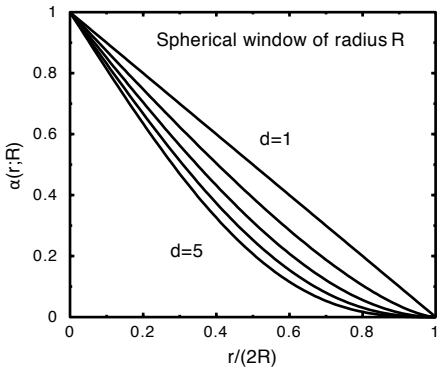

- For large R, we can show

$$\sigma^2(R) = 2^d\varphi\left[A\left(\frac{R}{D}\right)^d + B\left(\frac{R}{D}\right)^{d-1} + o\left(\frac{R}{D}\right)^{d-1}\right],$$

where A and B are the "volume" and "surface-area" coefficients:

$$A = S(\mathbf{k}=0) = 1 + \rho\int_{\mathbb{R}^d} h(\mathbf{r})d\mathbf{r}, \qquad B = -c(d)\int_{\mathbb{R}^d} h(\mathbf{r})r\,d\mathbf{r},$$

D: microscopic length scale, φ: dimensionless density

- **Hyperuniform**: $A = 0, B > 0$

INVERTED CRITICAL PHENOMENA: Ornstein-Zernike Formalism

- $h(\mathrm{r})$ can be divided into direct correlations, via function $c(\mathrm{r})$, and indirect correlations:

$$\tilde{c}(\mathrm{k}) = \frac{\tilde{h}(\mathrm{k})}{1 + \rho \tilde{h}(\mathrm{k})}$$

INVERTED CRITICAL PHENOMENA: Ornstein-Zernike Formalism

- $h(\mathrm{r})$ can be divided into direct correlations, via function $c(\mathrm{r})$, and indirect correlations:

$$\tilde{c}(\mathrm{k}) = \frac{\tilde{h}(\mathrm{k})}{1 + \rho \tilde{h}(\mathrm{k})}$$

- For any hyperuniform system, $\tilde{h}(\mathrm{k} = 0) = -1/\rho$, and thus $\tilde{c}(\mathrm{k} = 0) = -\infty$. Therefore, at the "critical" reduced density φ_c, $h(\mathrm{r})$ is short-ranged and $c(\mathrm{r})$ is long-ranged.

- This is the inverse of the behavior at liquid-gas (or magnetic) critical points, where $h(\mathrm{r})$ is long-ranged (compressibility or susceptibility diverges) and $c(\mathrm{r})$ is short-ranged.

INVERTED CRITICAL PHENOMENA: Ornstein-Zernike Formalism

- $h(\mathrm{r})$ can be divided into direct correlations, via function $c(\mathrm{r})$, and indirect correlations:

$$\tilde{c}(\mathrm{k}) = \frac{\tilde{h}(\mathrm{k})}{1 + \rho \tilde{h}(\mathrm{k})}$$

- For any hyperuniform system, $\tilde{h}(\mathrm{k} = 0) = -1/\rho$, and thus $\tilde{c}(\mathrm{k} = 0) = -\infty$. Therefore, at the "critical" reduced density φ_c, $h(\mathrm{r})$ is short-ranged and $c(\mathrm{r})$ is long-ranged.

- This is the inverse of the behavior at liquid-gas (or magnetic) critical points, where $h(\mathrm{r})$ is long-ranged (compressibility or susceptibility diverges) and $c(\mathrm{r})$ is short-ranged.

- For sufficiently large d at a disordered hyperuniform state, whether achieved via a nonequilibrium or an equilibrium route,

$$c(\mathrm{r}) \sim -\frac{1}{r^{d-2+\eta}} \quad (r \to \infty), \qquad \tilde{c}(\mathrm{k}) \sim -\frac{1}{k^{2-\eta}} \quad (k \to 0),$$

$$h(\mathrm{r}) \sim -\frac{1}{r^{d+2-\eta}} \quad (r \to \infty), \qquad S(\mathrm{k}) \sim k^{2-\eta} \quad (k \to 0),$$

where η is a new critical exponent.

- One can think of a hyperuniform system as one resulting from an effective pair potential $v(r)$ at large r that is a generalized Coulombic interaction between like charges. Why? Because

$$\frac{v(r)}{k_B T} \sim -c(r) \sim \frac{1}{r^{d-2+\eta}} \quad (r \to \infty)$$

- However, long-range interactions are not required to drive a nonequilibrium system to a disordered hyperuniform state.

SINGLE-CONFIGURATION FORMULATION & GROUND STATES

We showed

$$\sigma^2(R) = 2^d \varphi \left(\frac{R}{D}\right)^d \left[1 - 2^d \varphi \left(\frac{R}{D}\right)^d + \frac{1}{N} \sum_{i \neq j}^{N} \alpha(r_{ij}; R)\right]$$

where $\alpha(r;\ R)$ can be viewed as a repulsive pair potential:

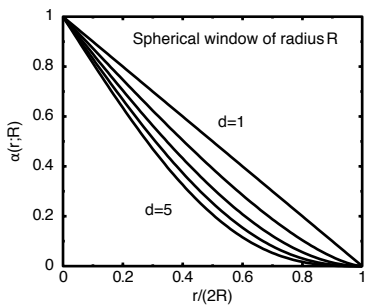

SINGLE-CONFIGURATION FORMULATION & GROUND STATES

- We showed

$$\sigma^2(R) = 2^d \varphi\left(\frac{R}{D}\right)\left[1 - 2^d \varphi\left(\frac{R}{D}\right) + \frac{1}{N}\sum_{i \neq j}^{N} \alpha(r_{ij}; R)\right]$$

where $\alpha(r;\ R)$ can be viewed as a repulsive pair potential:

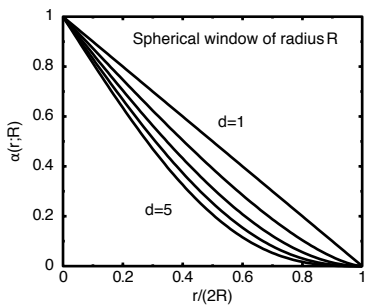

- Finding global minimum of $\sigma^2(R)$ equivalent to finding ground state.

SINGLE-CONFIGURATION FORMULATION & GROUND STATES

- We showed

$$\sigma^2(R) = 2^d\varphi \left(\frac{R}{D}\right)^d \left[1 - 2^d\varphi \left(\frac{R}{D}\right)^d + \frac{1}{N}\sum_{i\neq j}^{N} \alpha(r_{ij};R)\right]$$

where $\alpha(r;\ R)$ can be viewed as a repulsive pair potential:

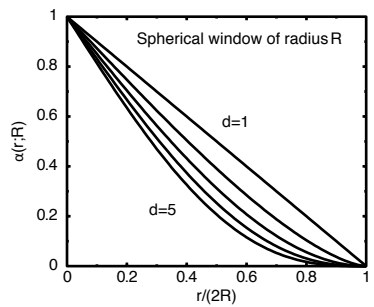

- Finding global minimum of $\sigma^2(R)$ equivalent to finding ground state.
- For large R, in the special case of hyperuniform systems,

$$\sigma^2(R) = \Lambda(R)\left(\frac{R}{D}\right)^{d-1} + O\left(\frac{R}{D}\right)^{d-3}$$

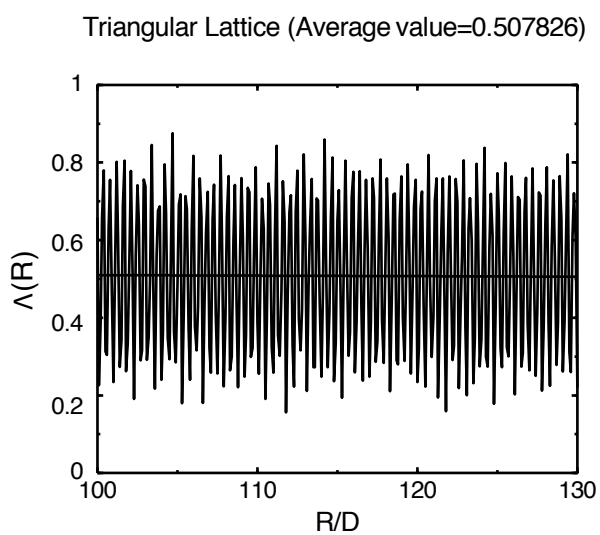

Hyperuniformity and Number Theory

- **Averaging fluctuating quantity $\Lambda(R)$ gives coefficient of interest:**

$$\overline{\Lambda} = \lim_{L \to \infty} \frac{1}{L} \int_0^L \Lambda(R)\,dR$$

Hyperuniformity and Number Theory

- **Averaging fluctuating quantity $\Lambda(R)$ gives coefficient of interest:**

$$\bar{\Lambda} = \lim_{L \to \infty} \frac{1}{L} \int_0^L \Lambda(R)\,dR$$

- **We showed that for a lattice**

$$\sigma^2(R) = \sum_{q \neq 0} \left(\frac{2\pi R}{q}\right)^d [J_{d/2}(qR)]^2, \qquad \bar{\Lambda} = 2^d \pi^{d-1} \sum_{q \neq 0} \frac{1}{|q|^{d+1}}.$$

- **Epstein zeta function for a lattice is defined by**

$$Z(s) = \sum_{q \neq 0} \frac{1}{|q|^{2s}}, \qquad \text{Re } s > d/2.$$

Summand can be viewed as an inverse power-law potential. For lattices, minimizer of $Z(d+1)$ is the lattice dual to the minimizer of $\bar{\Lambda}$.

- **Surface-area coefficient $\bar{\Lambda}$ provides useful way to rank order crystals, quasicrystals and special correlated disordered point patterns.**

Quantifying Suppression of Density Fluctuations at Large Scales: 1D

- The **surface-area coefficient** $\overline{\Lambda}$ for some **crystal, quasicrystal and disordered** one-dimensional hyperuniform point patterns.

Pattern	$\overline{\Lambda}$
Integer Lattice	$1/6 \approx 0.166667$
Step+Delta-Function g_2	3/16 =0.1875
Fibonacci Chain*	0.2011
Step-Function g_2	$1/4 = 0.25$
Randomized Lattice	$1/3 \approx 0.333333$

*Zachary & Torquato (2009)

Quantifying Suppression of Density Fluctuations at Large Scales: 2D

- The **surface-area coefficient** $\bar{\Lambda}$ for some **crystal, quasicrystal and disordered** two-dimensional hyperuniform point patterns.

2D Pattern	$\bar{\Lambda}/\varphi^{1/2}$
Triangular Lattice	0.508347
Square Lattice	0.516401
Honeycomb Lattice	0.567026
Kagome´ Lattice	0.586990
Penrose Tiling*	0.597798
Step+Delta-Function g_2	0.600211
Step-Function g_2	0.848826

*Zachary & Torquato (2009)

Quantifying Suppression of Density Fluctuations at Large Scales: 3D

- Contrary to conjecture that lattices associated with the densest sphere packings have smallest variance regardless of d, we have shown that for $d = 3$, BCC has a smaller variance than FCC.

Pattern	$\overline{\Lambda}/\varphi^{2/3}$
BCC Lattice	1.24476
FCC Lattice	1.24552
HCP Lattice	1.24569
SC Lattice	1.28920
Diamond Lattice	1.41892
Wurtzite Lattice	1.42184
Damped-Oscillating g_2	1.44837
Step+Delta-Function g_2	1.52686
Step-Function g_2	2.25

- Carried out analogous calculations in high d (Zachary & Torquato, 2009), of importance in communications. Disordered point patterns may win in high d (Torquato & Stillinger, 2006).

1D Translationally Invariant Hyperuniform Systems

- **An interesting 1D hyperuniform point pattern is the distribution of the nontrivial zeros of the Riemann zeta function (eigenvalues of random Hermitian matrices and bus arrivals in Cuernavaca): Dyson, 1970; Montgomery, 1973; Krba`lek & Šeba, 2000;** $g_2(r) = 1 - \sin^2(\pi r)/(\pi r)^2$

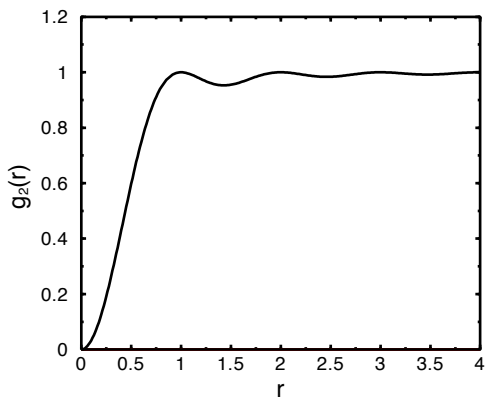

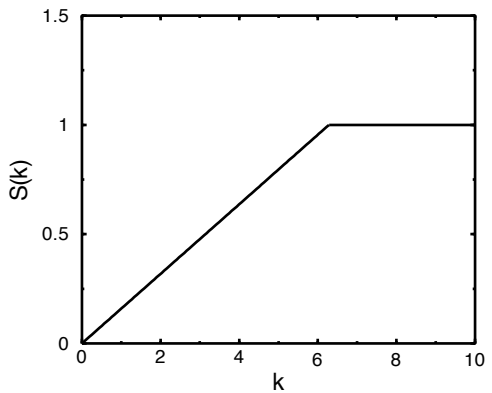

1D point process is always negatively correlated, i.e., $g_2(r) \leq 1$ **and pairs of points tend to repel one another, i.e.,** $g_2(r) \to 0$ **as** r **tends to zero.**

1D Translationally Invariant Hyperuniform Systems

- **An interesting 1D hyperuniform point pattern is the distribution of the nontrivial zeros of the Riemann zeta function (eigenvalues of random Hermitian matrices and bus arrivals in Cuernavaca): Dyson, 1970; Montgomery, 1973; Krbalek & Šeba, 2000;** $g_2(r) = 1 - \sin^2(\pi r)/(\pi r)^2$

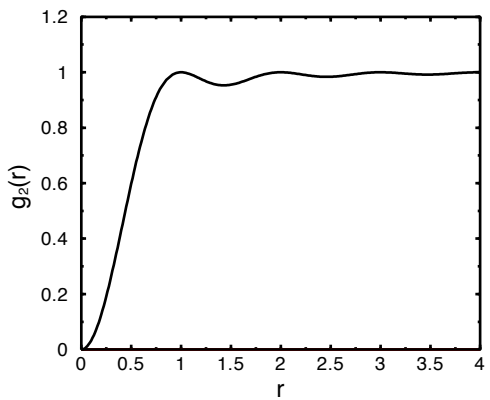

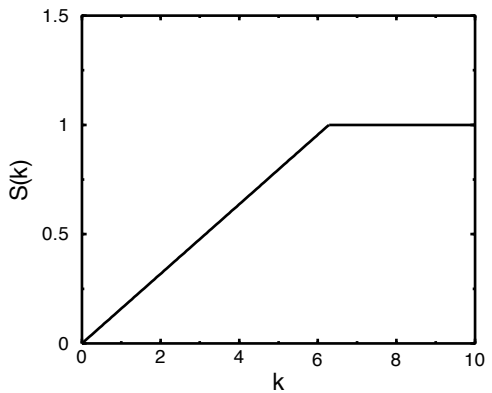

1D point process is always negatively correlated, i.e., $g_2(r) \leq 1$ **and pairs of points tend to repel one another, i.e.,** $g_2(r) \to 0$ **as** r **tends to zero.**

- **Dyson mapped this problem to a 1D log Coulomb gas at positive temperature:** $k_B T = 1/2$**. The total potential energy of the system is given by**

$$\Phi_N(\mathbf{r}^N) = \frac{1}{2}\sum_{i=1}^{N} |\mathbf{r}_i|^2 - \sum_{i \leq j}^{N} \ln(|\mathbf{r}_i - \mathbf{r}_j|).$$

1D Translationally Invariant Hyperuniform Systems

- An interesting 1D hyperuniform point pattern is the distribution of the nontrivial zeros of the Riemann zeta function (eigenvalues of random Hermitian matrices and bus arrivals in Cuernavaca): Dyson, 1970; Montgomery, 1973; Krbalek & Šeba, 2000; $g_2(r) = 1 - \sin^2(\pi r)/(\pi r)^2$

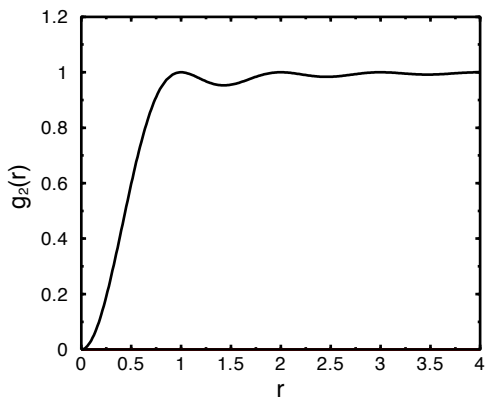

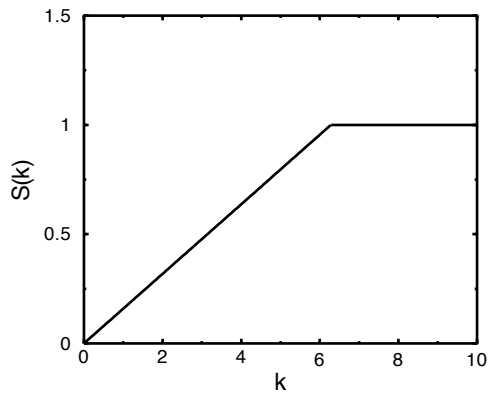

1D point process is always negatively correlated, i.e., $g_2(r) \leq 1$ and pairs of points tend to repel one another, i.e., $g_2(r) \to 0$ as r tends to zero.

- Dyson mapped this problem to a 1D log Coulomb gas at positive temperature: $k_B T = 1/2$. The total potential energy of the system is given by

$$\Phi_N(\mathbf{r}^N) = \frac{1}{2}\sum_{i=1}^{N} |\mathbf{r}_i|^2 - \sum_{i \leq j}^{N} \ln(|\mathbf{r}_i - \mathbf{r}_j|).$$

- Constructing and/or identifying homogeneous, isotropic hyperuniform patterns for $d \geq 2$ is more challenging. We now know of many more examples.

More Recent Examples of Disordered Hyperuniform Systems

- **Fermionic point processes**: $S(k) \sim k$ **as** $k \to 0$ **(ground states and/or positive temperature equilibrium states): Torquato et al. J. Stat. Mech. (2008)**
- **Maximally random jammed (MRJ) particle packings:** $S(k) \sim k$ **as** $k \to 0$ **(nonequilibrium states): Donev et al. PRL (2005)**
- **Ultracold atoms (nonequilibrium states): Lesanovsky et al. PRE (2014)**
- **Random organization (nonequilibrium states): Hexner et al. PRL (2015); Jack et al. PRL (2015); Weijs et. al. PRL (2015); Tjhung et al. PRL (2015)**
- **Disordered classical ground states: Uche et al. PRE (2004)**

More Recent Examples of Disordered Hyperuniform Systems

- **Fermionic point processes**: $S(k) \sim k$ as $k \to 0$ (ground states and/or positive temperature equilibrium states): Torquato et al. J. Stat. Mech. (2008)
- **Maximally random jammed** (MRJ) particle packings: $S(k) \sim k$ as $k \to 0$ (nonequilibrium states): Donev et al. PRL (2005)
- **Ultracold atoms** (nonequilibrium states): Lesanovsky et al. PRE (2014)
- **Random organization** (nonequilibrium states): Hexner et al. PRL (2015); Jack et al. PRL (2015); Weijs et. al. PRL (2015); Tjhung et al. PRL (2015)
- **Disordered classical ground states**: Uche et al. PRE (2004)

Natural Disordered Hyperuniform Systems

- **Avian Photoreceptors** (nonequilibrium states): Jiao et al. PRE (2014)
- **Immune-system receptors** (nonequilibrium states): Mayer et al. PNAS (2015)
- **Neuronal tracts** (nonequilibrium states): Burcaw et. al. NeuroImage (2015)

More Recent Examples of Disordered Hyperuniform Systems

- **Fermionic point processes**: $S(k) \sim k$ as $k \to 0$ (ground states and/or positive temperature equilibrium states): Torquato et al. J. Stat. Mech. (2008)
- **Maximally random jammed** (MRJ) particle packings: $S(k) \sim k$ as $k \to 0$ (nonequilibrium states): Donev et al. PRL (2005)
- **Ultracold atoms** (nonequilibrium states): Lesanovsky et al. PRE (2014)
- **Random organization** (nonequilibrium states): Hexner et al. PRL (2015); Jack et al. PRL (2015); Weijs et. al. PRL (2015); Tjhung et al. PRL (2015)
- **Disordered classical ground states**: Uche et al. PRE (2004)

Natural Disordered Hyperuniform Systems

- **Avian Photoreceptors** (nonequilibrium states): Jiao et al. PRE (2014)
- **Immune-system receptors** (nonequilibrium states): Mayer et al. PNAS (2015)
- **Neuronal tracts** (nonequilibrium states): Burcaw et. al. NeuroImage (2015)

Nearly Hyperuniform Disordered Systems

- **Amorphous Silicon** (nonequilibrium states): Henja et al. PRB (2013)
- **Structural Glasses** (nonequilibrium states): Marcotte et al. (2013)

Hyperuniformity and Spin-Polarized Free Fermions

- **One can map random Hermitian matrices (GUE), fermionic gases, and zeros of the Riemann zeta function to a unique hyperuniform point process on $\mathbb{R}$.**

Hyperuniformity and Spin-Polarized Free Fermions

- One can map random Hermitian matrices (GUE), fermionic gases, and zeros of the Riemann zeta function to a unique hyperuniform point process on $\mathbb{R}$.
- We provide exact generalizations of such a point process in d-dimensional Euclidean space $\mathbb{R}^d$ and the corresponding n-particle correlation functions, which correspond to those of spin-polarized free fermionic systems in $\mathbb{R}^d$.

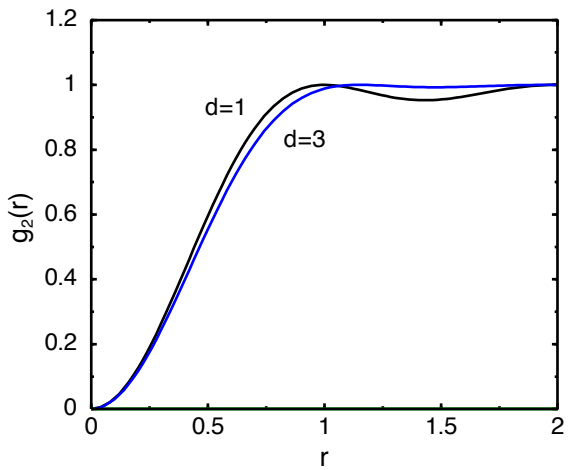

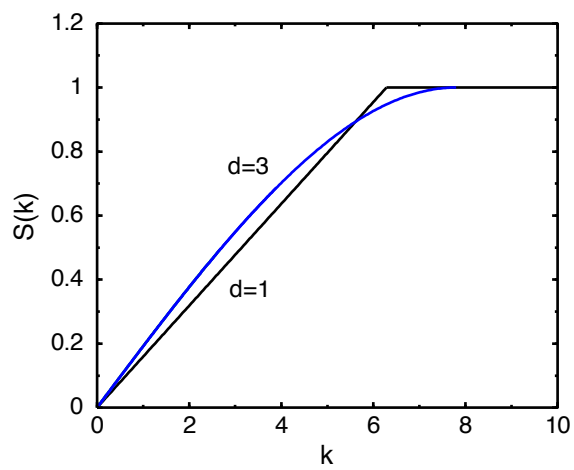

$$g_2(r) = 1 - \frac{2\Gamma(1 + d/2)\cos^2(rK - \pi(d+1)/4)}{K\pi^{d/2+1}\, r^{d+1}} \qquad (r \to \infty)$$

$$S(k) = \frac{c(d)}{2K}k + O(k^3) \qquad (k \to 0) \qquad (K : \text{Fermi sphere radius})$$

Torquato, Zachary & Scardicchio, J. Stat. Mech., 2008

Scardicchio, Zachary & Torquato, PRE, 2009

Hyperuniformity and Jammed Packings

- **Conjecture: All strictly jammed saturated sphere packings are hyperuniform (Torquato & Stillinger, 2003).**

Hyperuniformity and Jammed Packings

- **Conjecture: All strictly jammed saturated sphere packings are hyperuniform (Torquato & Stillinger, 2003).**
- **A 3D maximally random jammed (MRJ) packing is a prototypical glass in that it is maximally disordered but perfectly rigid (infinite elastic moduli).**
- **Such packings of identical spheres have been shown to be hyperuniform with quasi-long-range (QLR) pair correlations in which $h(r)$ decays as $-1/r^4$ (Donev, Stillinger & Torquato, PRL, 2005).**

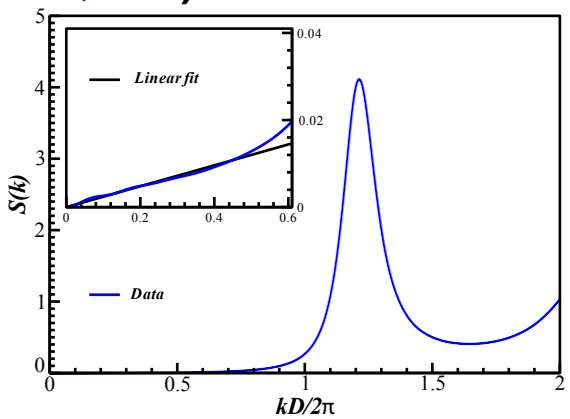

This is to be contrasted with the hard-sphere fluid with correlations that decay exponentially fast.

Hyperuniformity and Jammed Packings

- **Conjecture: All strictly jammed saturated sphere packings are hyperuniform (Torquato & Stillinger, 2003).**
- **A 3D maximally random jammed (MRJ) packing is a prototypical glass in that it is maximally disordered but perfectly rigid (infinite elastic moduli).**
- **Such packings of identical spheres have been shown to be hyperuniform with quasi-long-range (QLR) pair correlations in which $h(r)$ decays as $-1/r^4$ (Donev, Stillinger & Torquato, PRL, 2005).**

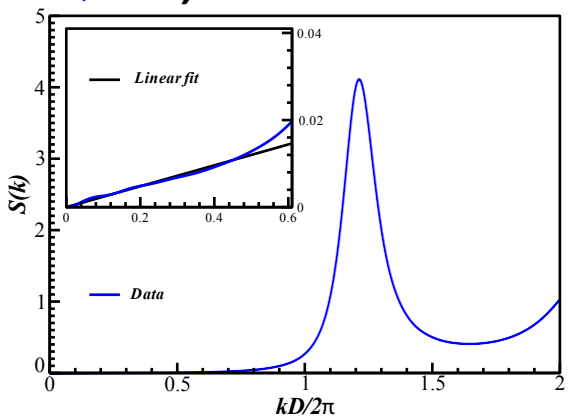

This is to be contrasted with the hard-sphere fluid with correlations that decay exponentially fast.

- **Apparently, hyperuniform QLR correlations with decay $-1/r^{d+1}$ are a universal feature of general MRJ packings in $\mathbb{R}^d$.**

  Zachary, Jiao and Torquato, PRL (2011): ellipsoids, superballs, sphere mixtures
  Berthier et al., PRL (2011); Kurita and Weeks, PRE (2011) : sphere mixtures Jiao and Torquato, PRE (2011): polyhedra

In the Eye of a Chicken: Photoreceptors

- **Optimal spatial sampling of light requires that photoreceptors be arranged in the triangular lattice (e.g., insects and some fish).**
- **Birds are highly visual animals, yet their cone photoreceptor patterns are irregular.**

In the Eye of a Chicken: Photoreceptors

- **Optimal** spatial sampling of light requires that **photoreceptors** be arranged in the **triangular lattice** (e.g., insects and some fish).
- **Birds** are highly **visual** animals, yet their cone photoreceptor patterns are **irregular**.

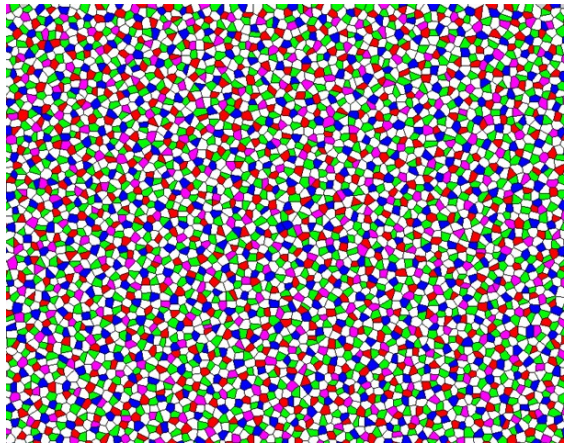

5 Cone Types

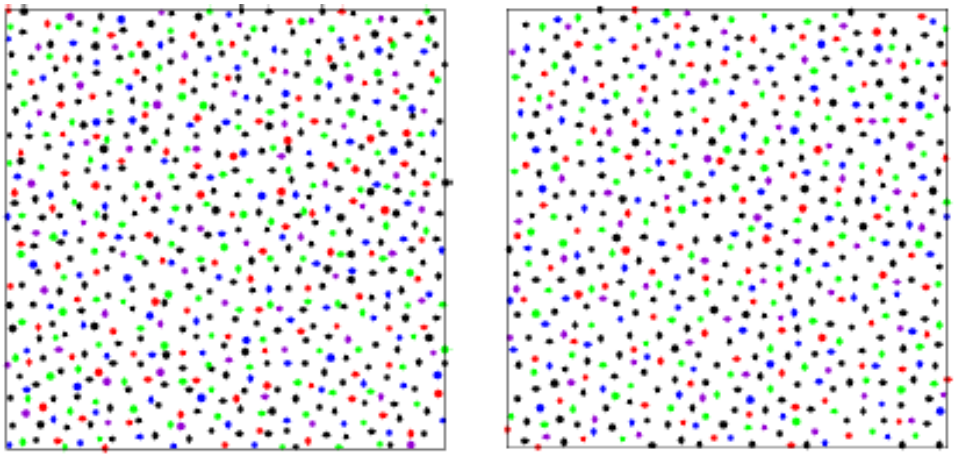

Jiao, Corbo & Torquato, PRE (2014).

Avian Cone Photoreceptors

- **Disordered mosaics of both total population and individual cone types are effectively hyperuniform, which has been never observed in any system before (biological or not). We term this multi-hyperuniformity.**

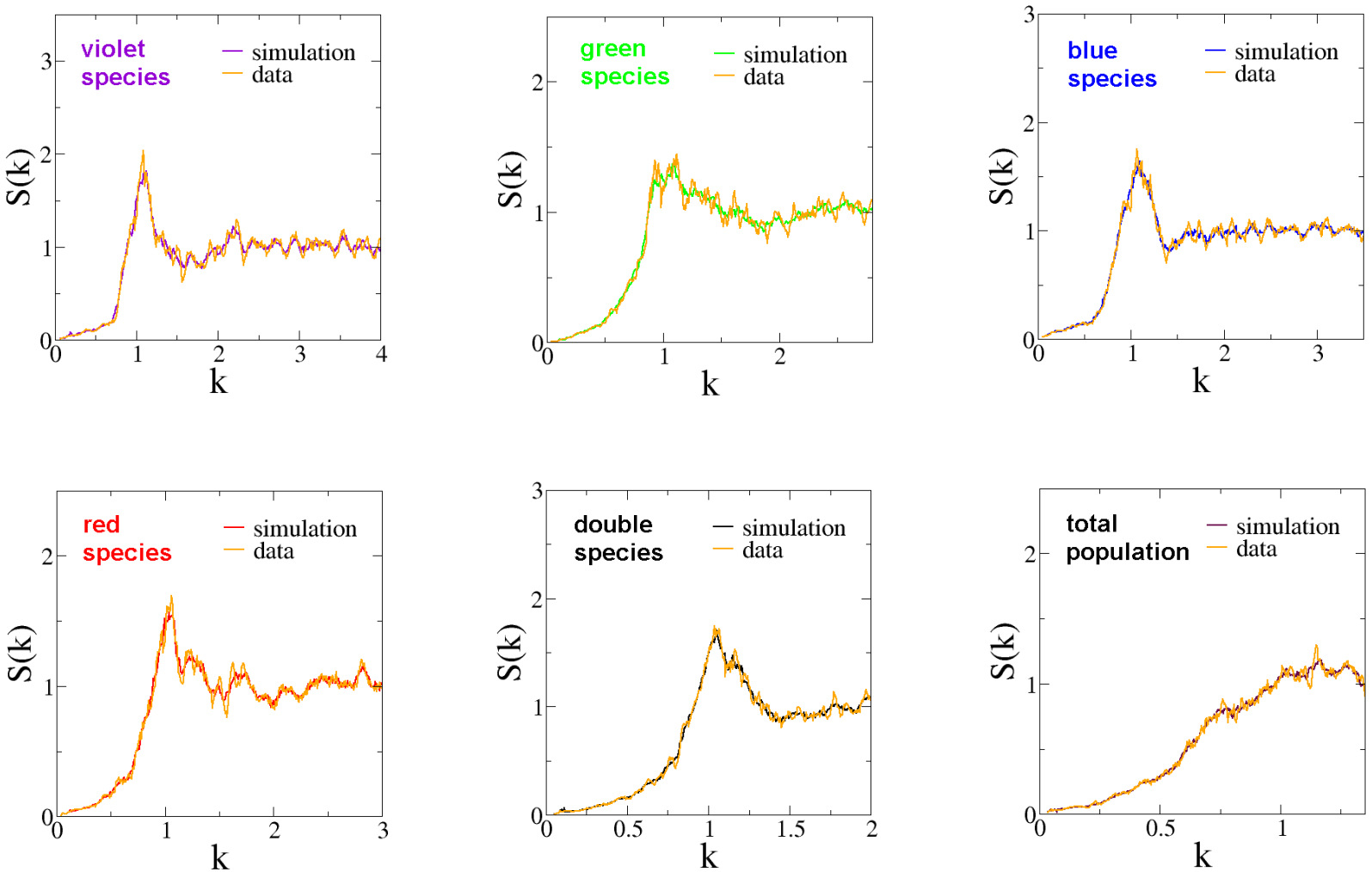

Jiao, Corbo & Torquato, PRE (2014)

Slow and Rapid Cooling of a Liquid

- **Classical ground states are those classical particle configurations with minimal potential energy per particle.**

Slow and Rapid Cooling of a Liquid

- Classical ground states are those classical particle configurations with minimal potential energy per particle.

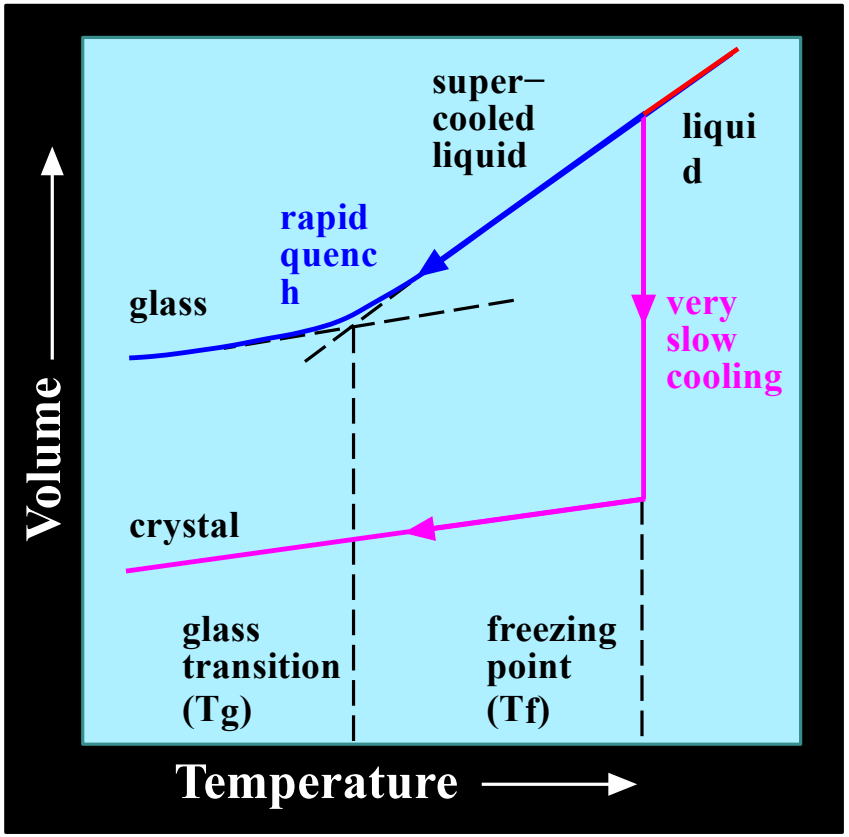

- Typically, ground states are periodic with high crystallographic symmetries.

Slow and Rapid Cooling of a Liquid

- Classical ground states are those classical particle configurations with minimal potential energy per particle.

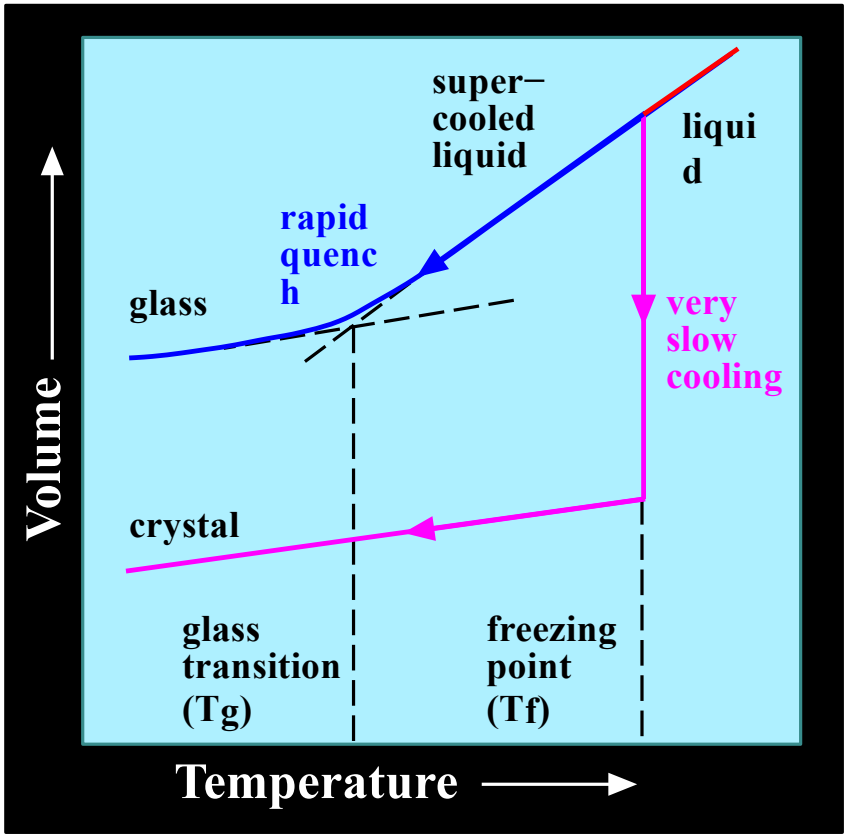

- Typically, ground states are periodic with high crystallographic symmetries.

- Can classical ground states ever be disordered?

Creation of Disordered Hyperuniform Ground States

Uche, Stillinger & Torquato, Phys. Rev. E 2004

Batten, Stillinger & Torquato, Phys. Rev. E 2008

Collective-Coordinate Simulations

•Consider a system of N particles with configuration r^N in a fundamental region Ω under periodic boundary conditions) with a pair potentials $v(\mathrm{r})$ that is bounded with Fourier transform $\tilde{v}(\mathrm{k})$.

Creation of Disordered Hyperuniform Ground States

Uche, Stillinger & Torquato, Phys. Rev. E 2004

Batten, Stillinger & Torquato, Phys. Rev. E 2008

Collective-Coordinate Simulations

•Consider a system of N particles with configuration r^N in a fundamental region Ω under periodic boundary conditions) with a pair potentials $v(\mathrm{r})$ that is bounded with Fourier transform $\tilde{v}(\mathrm{k})$.

The total energy is

$$\Phi_N(\mathrm{r}^N) = \sum_{i<j} v(\mathrm{r}_{ij})$$

$$= \frac{N}{2|\Omega|} \sum_k \tilde{v}(\mathrm{k}) S(\mathrm{k}) + \text{constant}$$

• For $\tilde{v}(\mathrm{k})$ positive $\forall\ 0 \leq |\mathrm{k}| \leq K$ and zero otherwise, finding configurations in which $S(\mathrm{k})$ is constrained to be zero where $\tilde{v}(\mathrm{k})$ has support is equivalent to globally minimizing $\Phi(\mathrm{r}^N)$.

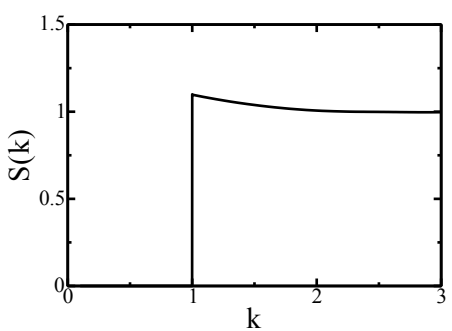

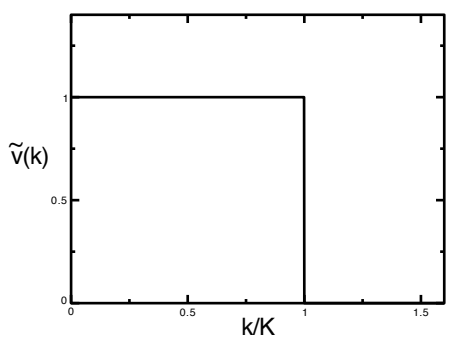

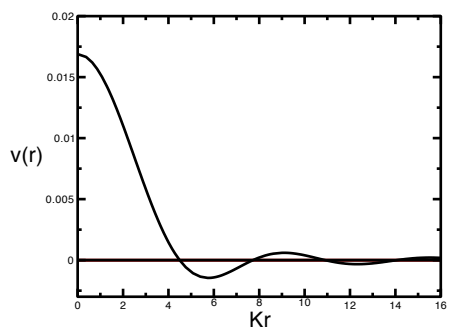

These hyperuniform ground states are called "stealthy" and generally highly degenerate.

Creation of Disordered Hyperuniform Ground States

Uche, Stillinger & Torquato, Phys. Rev. E 2004

Batten, Stillinger & Torquato, Phys. Rev. E 2008

Collective-Coordinate Simulations

•Consider a system of N particles with configuration r^N in a fundamental region Ω under periodic boundary conditions) with a pair potentials $v(\mathrm{r})$ that is bounded with Fourier transform $\tilde{v}(\mathrm{k})$.

The total energy is

$$\Phi_N(\mathrm{r}^N) = \sum_{i<j} v(\mathrm{r}_{ij})$$

$$= \frac{N}{2|\Omega|} \sum_k \tilde{v}(\mathrm{k}) S(\mathrm{k}) + \text{constant}$$

• For $\tilde{v}(\mathrm{k})$ positive $\forall\ 0 \leq |\mathrm{k}| \leq K$ and zero otherwise, finding configurations in which $S(\mathrm{k})$ is constrained to be zero where $\tilde{v}(\mathrm{k})$ has support is equivalent to globally minimizing $\Phi(\mathrm{r}^N)$.

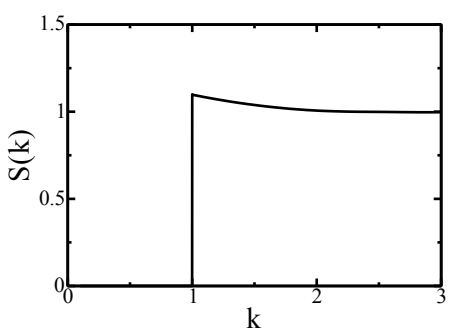

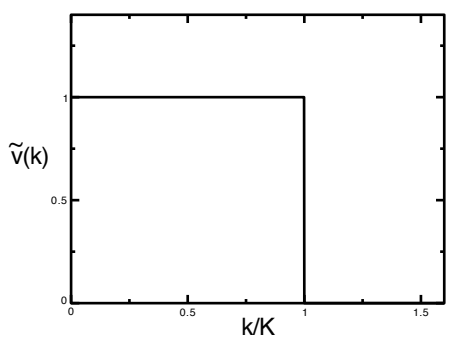

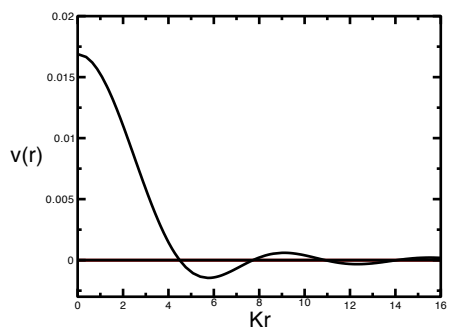

These hyperuniform ground states are called "stealthy" and generally highly degenerate.

•Stealthy patterns can be tuned by varying the parameter χ: ratio of number of constrained degrees of freedom to the total number of degrees of freedom, $d(N-1)$.

- **Previously, started with an initial random distribution of N points and then found the energy minimizing configurations (with extremely high precision) using optimization techniques.**

Creation of Disordered Stealthy Ground States

Creation of Disordered Stealthy Ground States

- **Previously, started with an initial random distribution of N points and then found the energy minimizing configurations (with extremely high precision) using optimization techniques.**
- **For $0 \leq \chi < 0.5$, the stealthy ground states are degenerate, disordered and isotropic.**

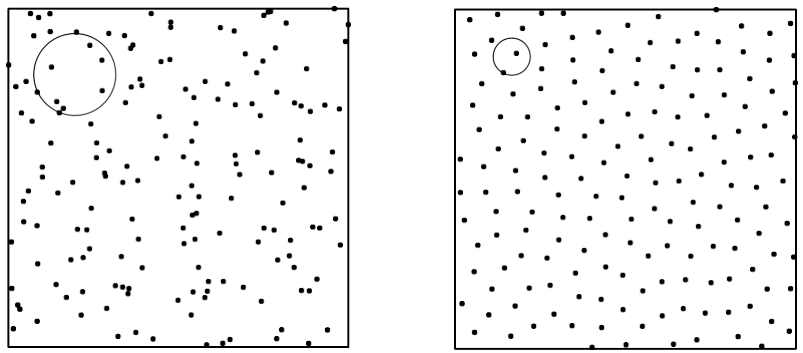

(a) $\chi = 0.04167$ (b) $\chi = 0.41071$

- **Success rate to achieve disordered ground states is 100%.**

Creation of Disordered Stealthy Ground States

- **Previously, started with an initial random distribution of N points and then found the energy minimizing configurations (with extremely high precision) using optimization techniques.**
- **For $0 \leq \chi < 0.5$, the stealthy ground states are degenerate, disordered and isotropic.**

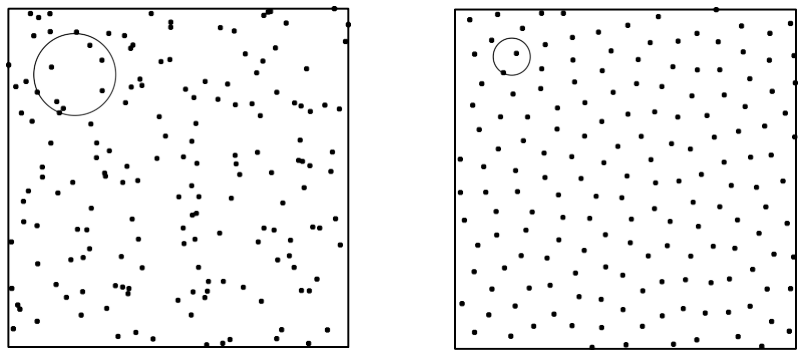

(a) $\chi = 0.04167$ (b) $\chi = 0.41071$

- **Success rate to achieve disordered ground states is 100%.**
- **For $\chi > 1/2$, the system undergoes a transition to a crystal phase and the energy landscape becomes considerably more complex.**

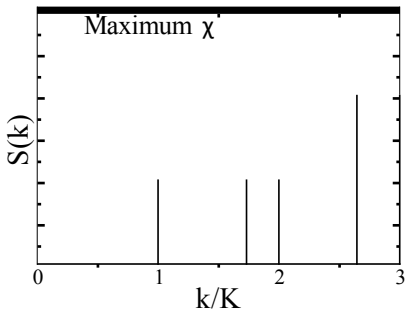

Animations

Stealthy Disordered Ground States and Novel Materials

- **Until recently, it was believed that Bragg scattering was required to achieve metamaterials with complete photonic band gaps.**

Stealthy Disordered Ground States and Novel Materials

- Until recently, it was believed that Bragg scattering was required to achieve metamaterials with complete photonic band gaps.
- Have used disordered, isotropic "stealthy" ground-state configurations to design photonic materials with large complete (both polarizations and all directions) band gaps.

Florescu, Torquato and Steinhardt, PNAS (2009)

Stealthy Disordered Ground States and Novel Materials

- Until recently, it was believed that Bragg scattering was required to achieve metamaterials with complete photonic band gaps.
- Have used disordered, isotropic "stealthy" ground-state configurations to design photonic materials with large complete (both polarizations and all directions) band gaps.

  Florescu, Torquato and Steinhardt, PNAS (2009)

- These network material designs have been fabricated for microwave regime.

  Man et. al., PNAS (2013)

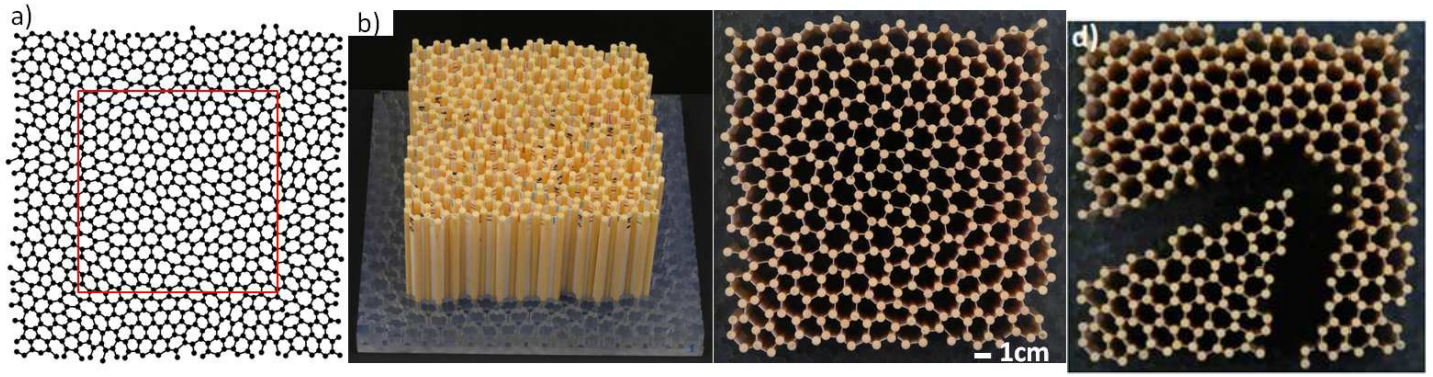

Because band gaps are isotropic, such photonic materials offer advantages over photonic crystals (e.g., free-form waveguides).

Stealthy Disordered Ground States and Novel Materials

- Until recently, it was believed that Bragg scattering was required to achieve metamaterials with complete photonic band gaps.
- Have used disordered, isotropic "stealthy" ground-state configurations to design photonic materials with large complete (both polarizations and all directions) band gaps.

  Florescu, Torquato and Steinhardt, PNAS (2009)

- These network material designs have been fabricated for microwave regime.

  Man et. al., PNAS (2013)

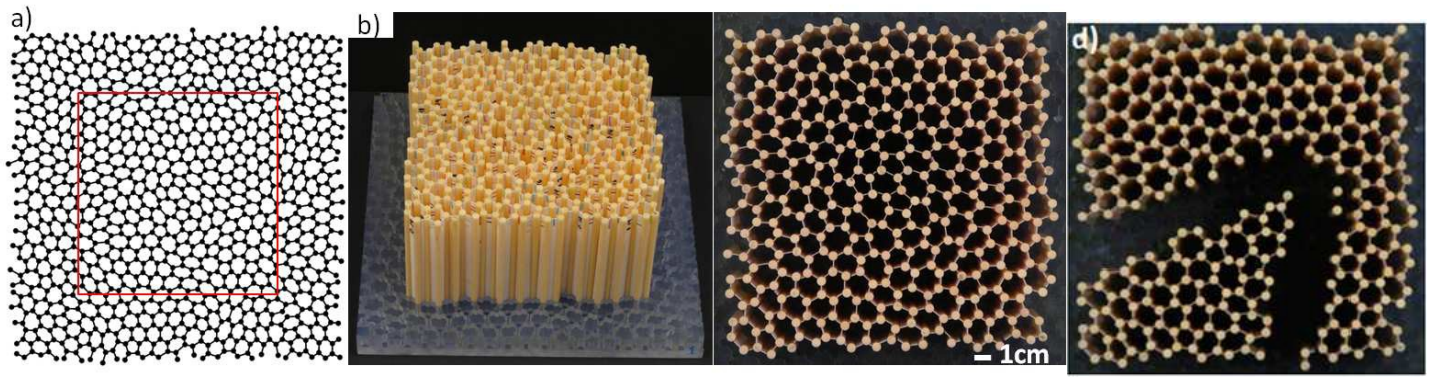

Because band gaps are isotropic, such photonic materials offer advantages over photonic crystals (e.g., free-form waveguides).

- High-density transparent stealthy disordered materials: Leseur, Pierrat & Carminati (2016).

Ensemble Theory of Disordered Ground States

Torquato, Zhang & Stillinger, Phys. Rev. X, 2015

- **Nontrivial**: Dimensionality of the configuration space depends on the number density ρ (or χ) and there is a multitude of ways of sampling the ground-state manifold, each with its own probability measure. **Which ensemble?** How are **entropically favored** states determined?
- Derived general exact relations for thermodynamic properties that apply to any ground-state ensemble as a function of ρ in any d and showed how disordered degenerate ground states arise.

Ensemble Theory of Disordered Ground States

Torquato, Zhang & Stillinger, Phys. Rev. X, 2015

- **Nontrivial**: Dimensionality of the configuration space depends on the number density ρ (or χ) and there is a multitude of ways of sampling the ground-state manifold, each with its own probability measure. **Which ensemble?** How are **entropically favored** states determined?
- Derived general exact relations for thermodynamic properties that apply to any ground-state ensemble as a function of ρ in any d and showed how disordered degenerate ground states arise.
- From previous considerations, we that an important contribution to $S(k)$ is a simple hard-core step function $\Theta(k - K)$, which can be viewed as a **disordered hard-sphere system in Fourier space** in the limit that $\chi \sim 1/\rho$ tends to zero, i.e., as the number density ρ tends to infinity.

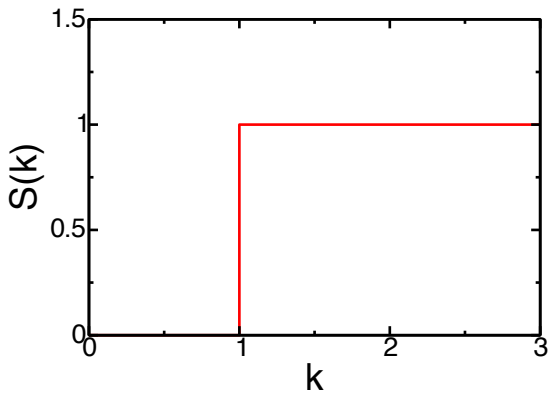

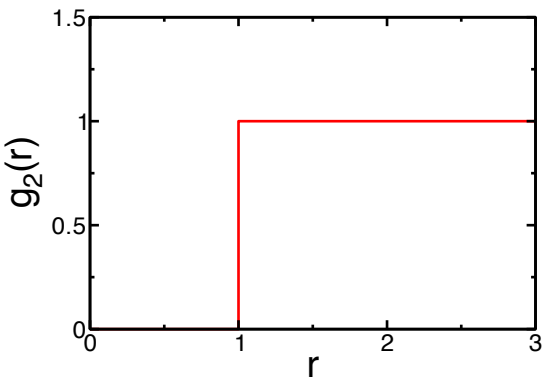

- That the structure factor must have the behavior

$$S(k) \to \Theta(k - K), \qquad \chi \to 0$$

is perfectly reasonable; it is a **perturbation about the ideal-gas limit in which $S(k) = 1$ for all k**.

Ensemble Theory of Disordered Ground States

Torquato, Zhang & Stillinger, Phys. Rev. X, 2015

- **Nontrivial**: Dimensionality of the configuration space depends on the number density ρ (or χ) and there is a multitude of ways of sampling the ground-state manifold, each with its own probability measure. **Which ensemble?** How are **entropically favored** states determined?
- Derived general exact relations for thermodynamic properties that apply to any ground-state ensemble as a function of ρ in any d and showed how disordered degenerate ground states arise.
- From previous considerations, we that an important contribution to $S(k)$ is a simple hard-core step function $\Theta(k - K)$, which can be viewed as a **disordered hard-sphere system in Fourier space** in the limit that $\chi \sim 1/\rho$ tends to zero, i.e., as the number density ρ tends to infinity.

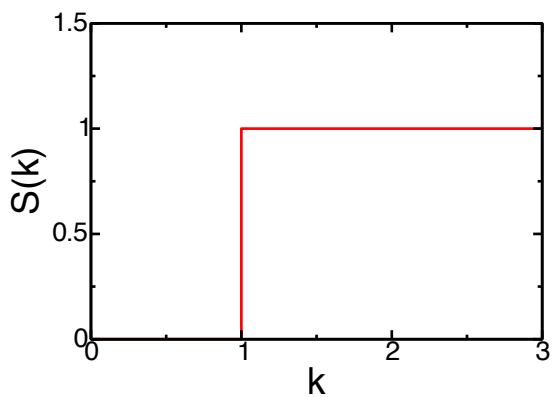

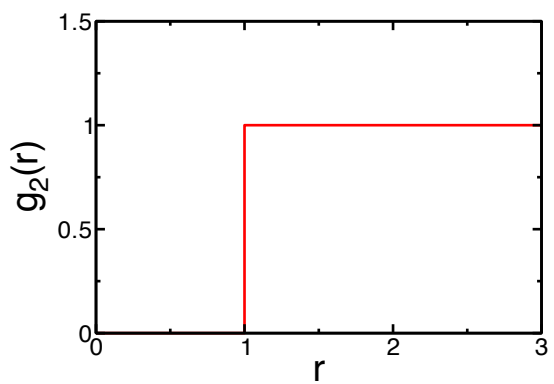

- That the structure factor must have the behavior

$$S(k) \to \Theta(k - K), \qquad \chi \to 0$$

is perfectly reasonable; it is a **perturbation about the ideal-gas limit in which $S(k) = 1$ for all k**.

- We make the **ansatz** that for sufficiently small χ, $S(k)$ in the **canonical ensemble** for a stealthy potential can be mapped to $g_2(r)$ for an **effective disordered hard-sphere system for sufficiently small density**.

Pseudo-Hard Spheres in Fourier Space

Let us define

$$\tilde{H}(k) \equiv \rho \tilde{h}(k) = h_{HS}(r = k)$$

There is an Ornstein-Zernike integral eq. that defines FT of appropriate direct correlation function, $\tilde{C}(k)$**:**

$$\tilde{H}(k) = \tilde{C}(k) + \eta \tilde{H}(k) \otimes \tilde{C}(k),$$

where η **is an effective packing fraction. Therefore,**

$$H(r) = \frac{C(r)}{1 - (2\pi)^d \eta C(r)}.$$

This mapping enables us to exploit the well-developed accurate theories of standard Gibbsian disordered hard spheres in direct space.

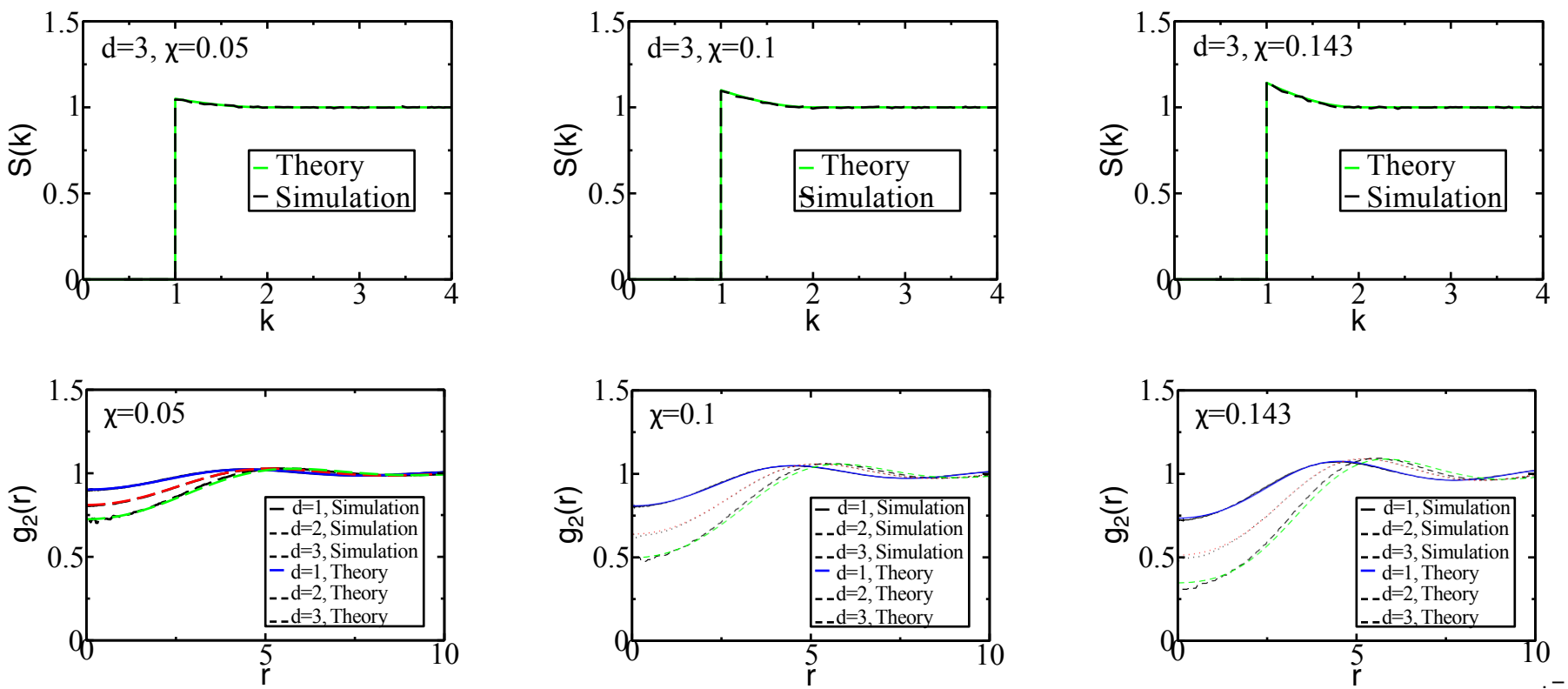

General Scaling Behaviors

- **Hyperuniform particle distributions possess structure factors with a small-wavenumber scaling**

$$S(k) \sim k^{\alpha}, \qquad \alpha > 0,$$

including the special case $\alpha = +\infty$ for periodic crystals.

- **Hence, number variance $\sigma^2(R)$ increases for large R asymptotically as (Zachary and Torquato, 2011)**

$$\sigma^2(R) \sim \begin{cases} R^{d-1} \ln R, & \alpha = 1 \\ R^{d-\alpha}, & \alpha < 1 \\ R^{d-1}, & \alpha > 1 \end{cases} \qquad (R \to +\infty).$$

- **Until recently, all known hyperuniform configurations pertained to $\alpha \geq 1$.**

Targeted Spectra $S \sim k^{\alpha}$

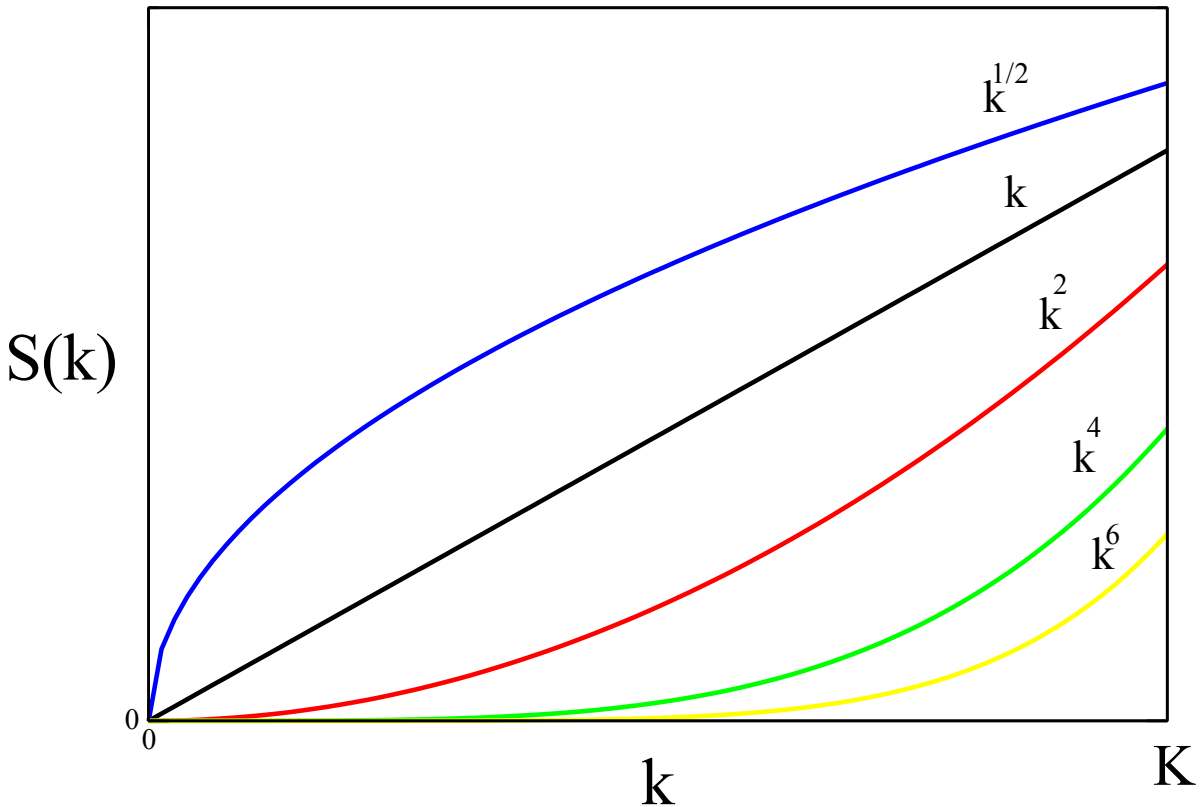

- **Configurations are ground states of an interacting many-particle system with up to four-body interactions.**

Targeted Spectra $S \sim k^{\alpha}$ with $\alpha \geq 1$

Uche, Stillinger & Torquato (2006)

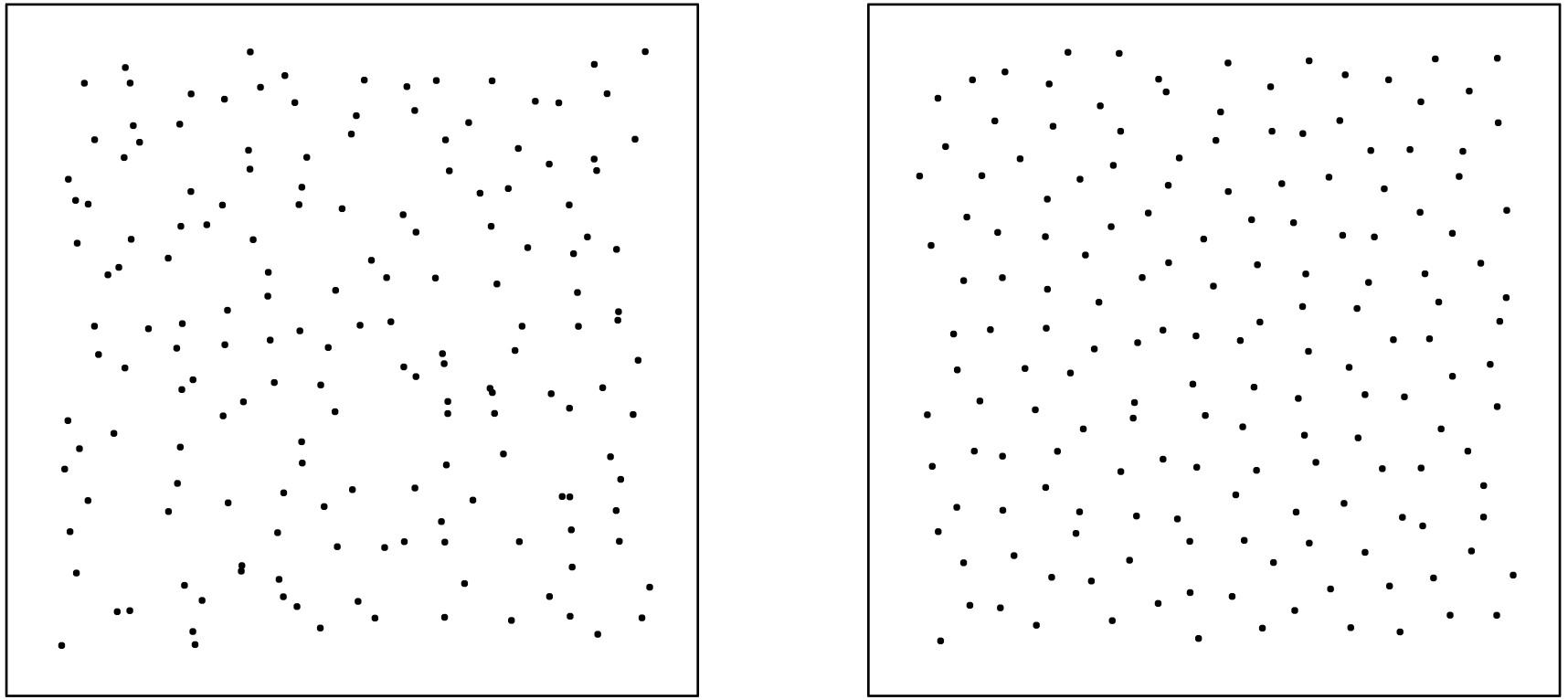

Figure 1: One of them is for $S(k) \sim k^6$ and other for $S(k) \sim k$.

Targeted Spectra $S \sim k^{\alpha}$ with $\alpha < 1$

Zachary & Torquato (2011)

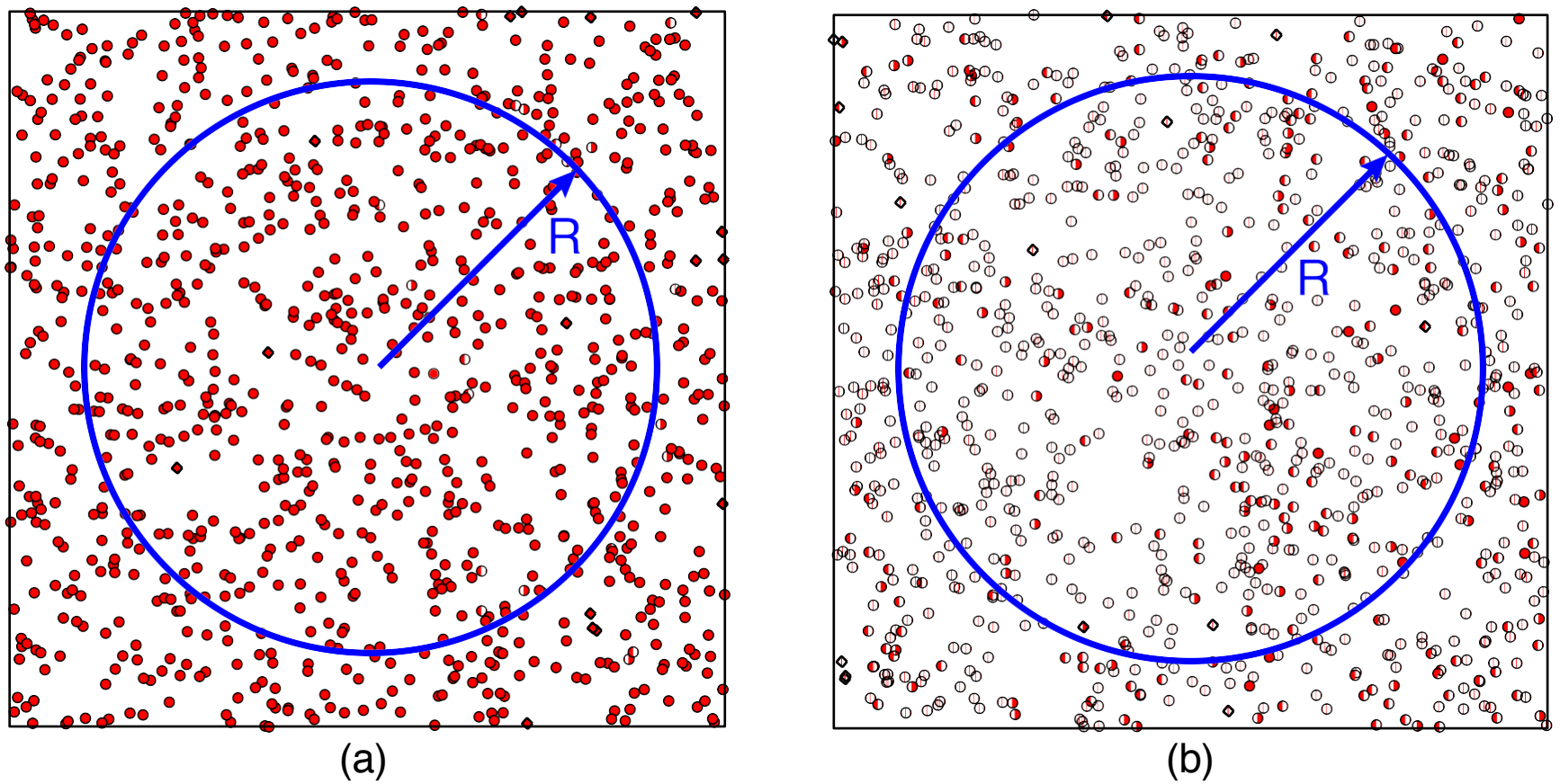

Figure 2: **Both configurations exhibit strong local clustering of points and possess a highly irregular local structure; however, only one of them is hyperuniform (with $S \sim k^{1/2}$).**

Amorphous Silicon is Nearly Hyperuniform

- **Highly sensitive transmission X-ray scattering measurements performed at Argonne on amorphous-silicon (a-Si) samples reveals that they are nearly hyperuniform with $S(0) = 0.0075$.**

  Long, Roorda, Hejna, Torquato, and Steinhardt (2013)

- **This is significantly below the putative lower bound recently suggested by de Graff and Thorpe (2009) but consistent with the recently proposed nearly hyperuniform network picture of a-Si (Hejna, Steinhardt and Torquato, 2013).**

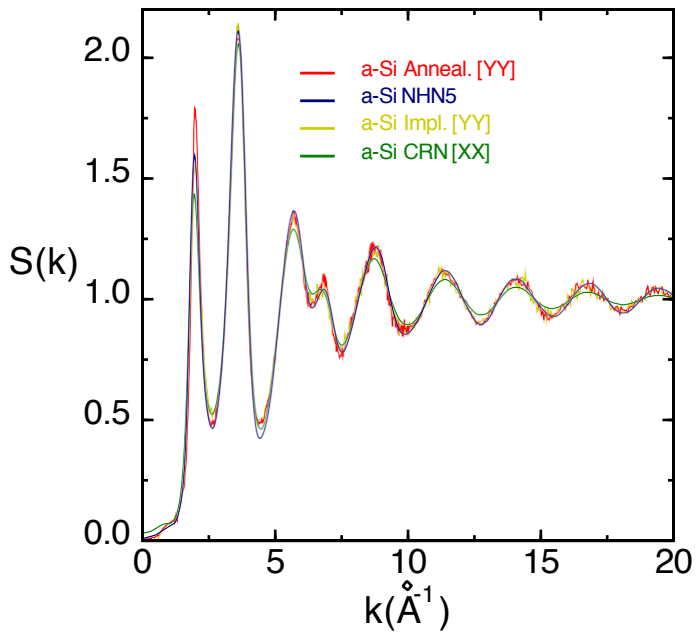

Amorphous Silicon is Nearly Hyperuniform

- **Highly sensitive transmission X-ray scattering measurements performed at Argonne on amorphous-silicon (a-Si) samples reveals that they are nearly hyperuniform with $S(0) = 0.0075$.**

  Long, Roorda, Hejna, Torquato, and Steinhardt (2013)

- **This is significantly below the putative lower bound recently suggested by de Graff and Thorpe (2009) but consistent with the recently proposed nearly hyperuniform network picture of a-Si (Hejna, Steinhardt and Torquato, 2013).**

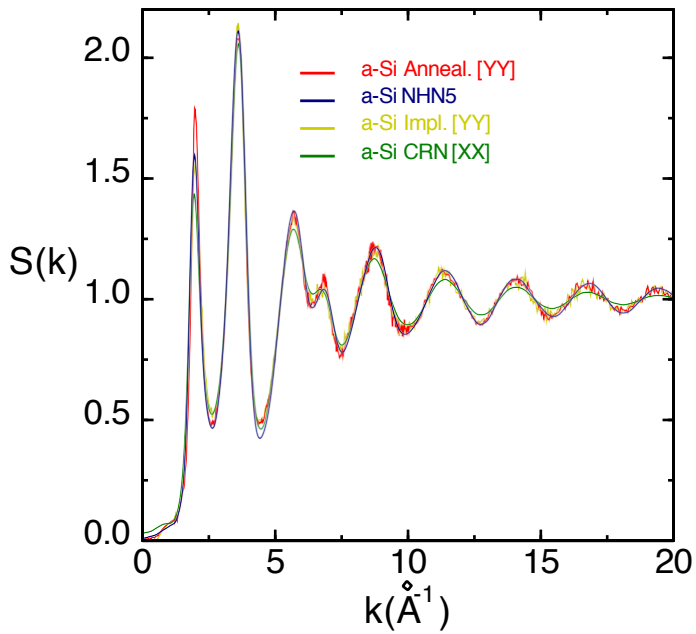

- **Increasing the degree of hyperuniformity of a-Si appears to be correlated with a larger electronic band gap (Hejna, Steinhardt and Torquato, 2013).**

Structural Glasses and Growing Length Scales

- **Important question in glass physics: Do growing relaxation times under supercooling have accompanying growing structural length scales?** Lubchenko & Wolynes (2006); Berthier et al. (2007); Karmakar, Dasgupta & Sastry (2009); Chandler & Garrahan (2010); Hocky, Markland & Reichman (2012)

Structural Glasses and Growing Length Scales

- **Important question in glass physics: Do growing relaxation times under supercooling have accompanying growing structural length scales?** Lubchenko & Wolynes (2006); Berthier et al. (2007); Karmakar, Dasgupta & Sastry (2009); Chandler & Garrahan (2010); Hocky, Markland & Reichman (2012)

- **We studied glass-forming liquid models that support an alternative view: existence of growing static length scales (due to increase of the degree of hyperuniformity) as the temperature T of the supercooled liquid is decreased to and below T_g that is intrinsically nonequilibrium in nature.**

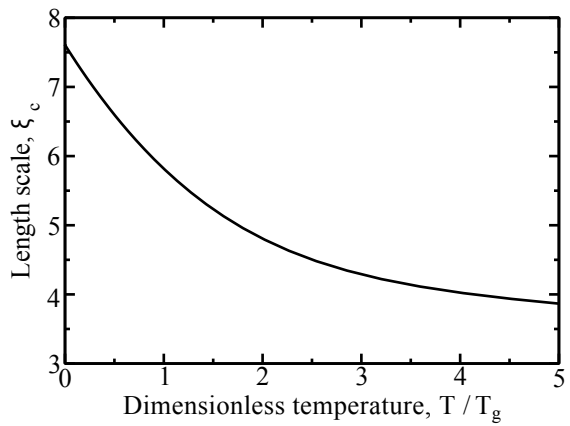

Structural Glasses and Growing Length Scales

- Important question in glass physics: Do growing relaxation times under supercooling have accompanying growing structural length scales? Lubchenko & Wolynes (2006); Berthier et al. (2007); Karmakar, Dasgupta & Sastry (2009); Chandler & Garrahan (2010); Hocky, Markland & Reichman (2012)

- We studied glass-forming liquid models that support an alternative view: existence of growing static length scales (due to increase of the degree of hyperuniformity) as the temperature T of the supercooled liquid is decreased to and below T_g that is intrinsically nonequilibrium in nature.

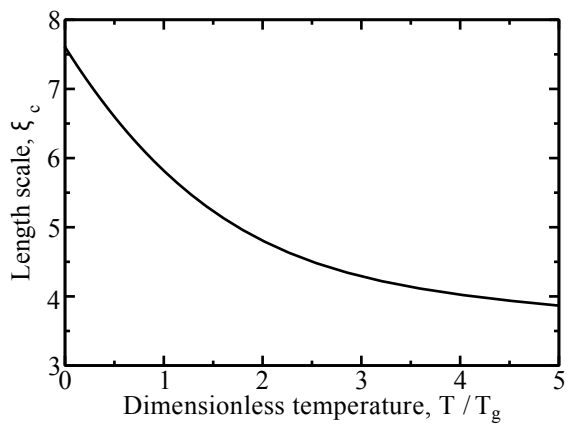

- The degree of deviation from thermal equilibrium is determined from a nonequilibrium index

$$X = \frac{S(k=0)}{\rho k_B T \kappa_T} - 1,$$

which increases upon supercooling.

Marcotte, Stillinger & Torquato (2013)

- **Hyperuniformity concept was generalized to the case of heterogeneous materials: phase volume fraction fluctuates within a spherical window of radius R (Zachary and Torquato, 2009).**

Hyperuniformity of 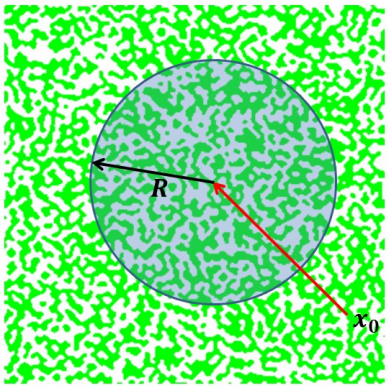 vo-Phase Materials

Hyperuniformity of Disordered Two-Phase Materials

- Hyperuniformity concept was generalized to the case of heterogeneous materials: phase volume fraction fluctuates within a spherical window of radius R (Zachary and Torquato, 2009).

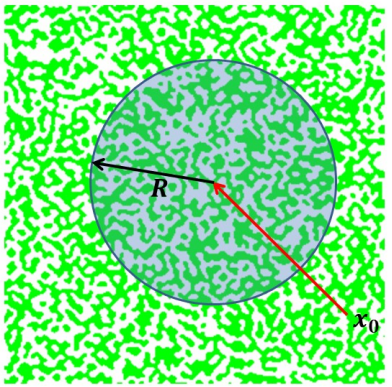

- For typical disordered media, volume-fraction variance $\sigma_v^2(R)$ for large R goes to zero like R^{-d}.
- For hyperuniform disordered two-phase media, $\sigma_v^2(R)$ goes to zero faster than R^{-d}, equivalent to following condition on spectral density $\tilde{\chi}_v(\mathrm{k})$:

$$\lim_{|k| \to 0} \tilde{\chi}_v(\mathrm{k}) = 0.$$

Hyperuniformity of Disordered Two-Phase Materials

- Hyperuniformity concept was generalized to the case of heterogeneous materials: phase volume fraction fluctuates within a spherical window of radius R (Zachary and Torquato, 2009).

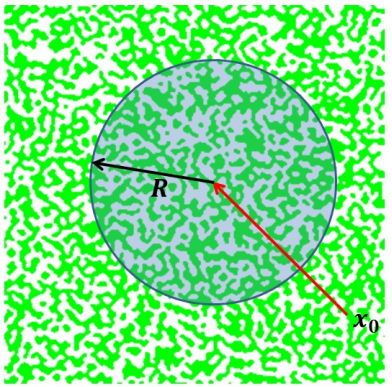

- For typical disordered media, volume-fraction variance $\sigma_v^2(R)$ for large R goes to zero like R^{-d}.
- For hyperuniform disordered two-phase media, $\sigma_v^2(R)$ goes to zero faster than R^{-d}, equivalent to following condition on spectral density $\tilde{\chi}_v(\mathrm{k})$:

$$\lim_{|k|\to 0} \tilde{\chi}_v(\mathrm{k}) = 0.$$

- Interfacial-area fluctuations play an important role in static and surface-area evolving structures. Here we define $\sigma_s^2(R)$ and hyperuniformity condition is (Torquato, PRE, 2016)

$$\lim_{|k|\to 0} \tilde{\chi}_s(\mathrm{k}) = 0.$$

Designing Disordered Hyperuniform Heterogeneous Materials

- **Disordered hyperuniform two-phase systems can be designed with targeted spectral functions (Torquato, J. Phys.: Cond. Mat., 2016).**

- **For example, consider the following hyperuniform functional forms in 2D and 3D:**

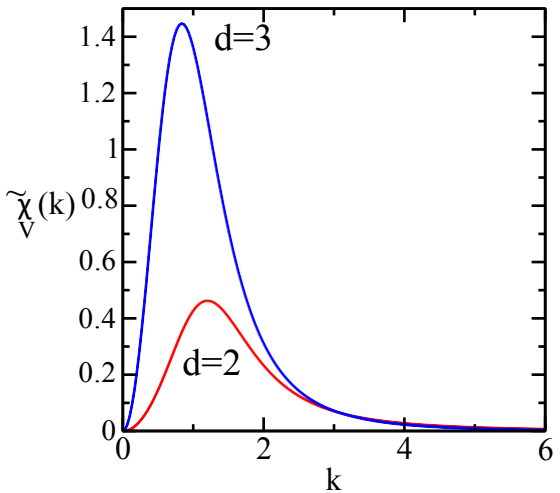

Designing Disordered Hyperuniform Heterogeneous Materials

- **Disordered hyperuniform two-phase systems can be designed with targeted spectral functions (Torquato, J. Phys.: Cond. Mat., 2016).**

- **For example, consider the following hyperuniform functional forms in 2D and 3D:**

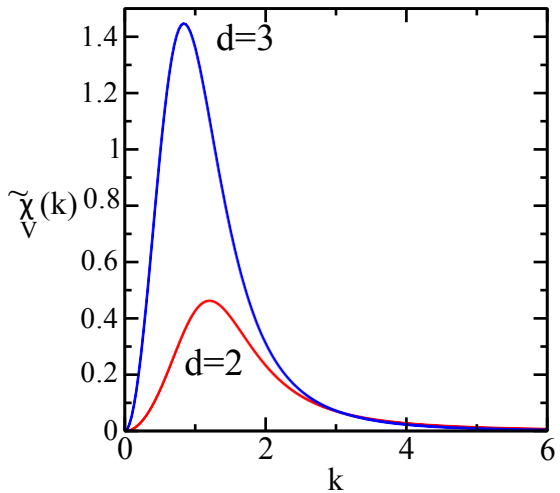

- **The following is a 2D realization:**

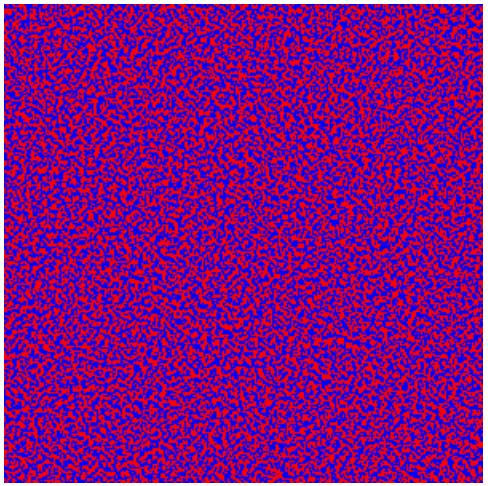

Other Generalization of Hyperuniformity

- Consider
  - Random scalar fields: Concentration and temperature fields in random media and turbulent flows, laser speckle patterns, and temperature fluctuations associated with CMB.
  - Random vector fields: Random media (e.g., heat, current, electric, magnetic and velocity vector fields) and turbulence.
  - Structurally anisotropic materials: Many-particle systems and random media that are statistically anisotropic.

Other Generalization of Hyperuniformity

- **Consider**
  - **Random scalar fields: Concentration and temperature fields in random media and turbulent flows, laser speckle patterns, and temperature fluctuations associated with CMB.**
  - **Random vector fields: Random media (e.g., heat, current, electric, magnetic and velocity vector fields) and turbulence.**
  - **Structurally anisotropic materials: Many-particle systems and random media that are statistically anisotropic.**
- **Directional hyperuniformity: For unit vector $\mathbf{k}_Q$ and scalar t,**

$$\lim_{t \to 0} \tilde{\Psi}_{ij}(t\mathbf{k}_Q) = 0$$

Other Generalization of Hyperuniformity

- Consider
  - **Random scalar fields**: Concentration and temperature fields in random media and turbulent flows, laser speckle patterns, and temperature fluctuations associated with CMB.
  - **Random vector fields**: Random media (e.g., heat, current, electric, magnetic and velocity vector fields) and turbulence.
  - **Structurally anisotropic materials**: Many-particle systems and random media that are statistically anisotropic.
- **Directional hyperuniformity**: For unit vector $\mathbf{k}_Q$ and scalar t,

$$\lim_{t \to 0} \tilde{\Psi}_{ij}(t\mathbf{k}_Q) = 0$$

- Is there a many-particle system with following **anisotropic scattering pattern?**

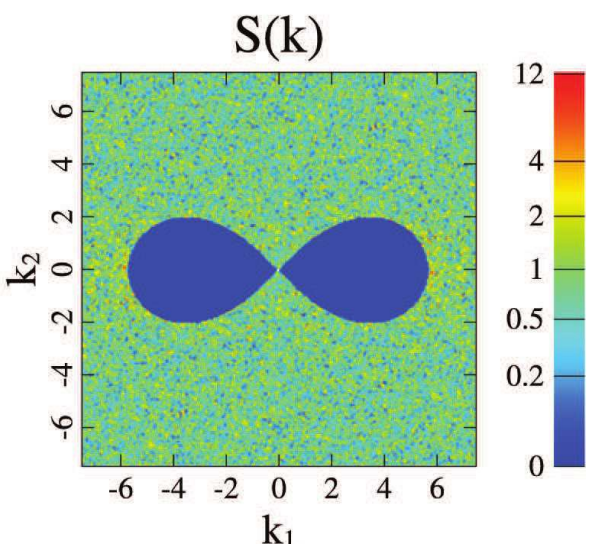

Other Generalization of Hyperuniformity

- Consider
  - Random scalar fields: Concentration and temperature fields in random media and turbulent flows, laser speckle patterns, and temperature fluctuations associated with CMB.
  - Random vector fields: Random media (e.g., heat, current, electric, magnetic and velocity vector fields) and turbulence.
  - Structurally anisotropic materials: Many-particle systems and random media that are statistically anisotropic.
- Directional hyperuniformity: For unit vector $\mathbf{k}_Q$ and scalar t,

$$\lim_{t \to 0} \tilde{\Psi}_{ij}(t\mathbf{k}_Q) = 0$$

- Is there a many-particle system with following anisotropic scattering pattern?

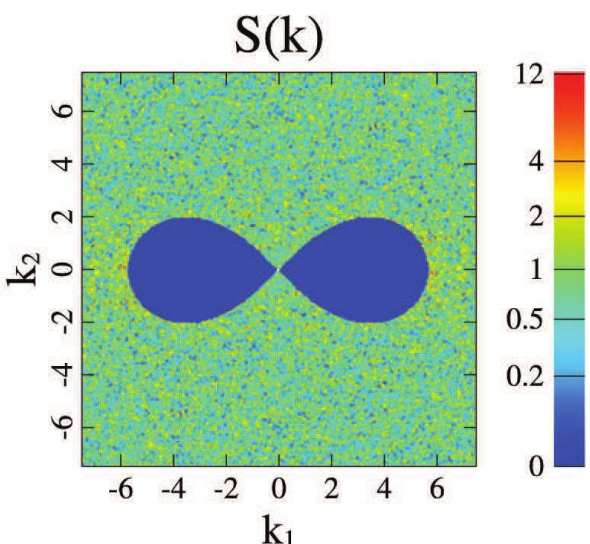

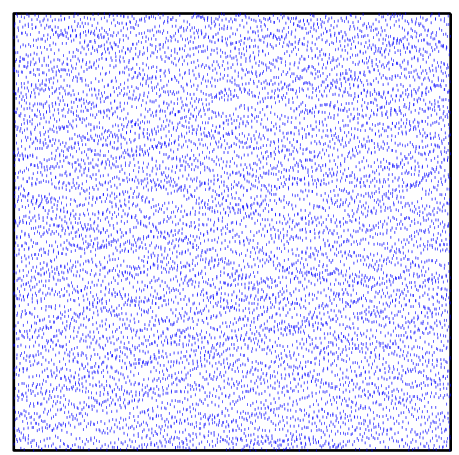

CONCLUSIONS

- **Disordered hyperuniform materials are new ideal states of disordered matter.**
- **Hyperuniformity provides a unified means of categorizing and characterizing crystals, quasicrystals and special correlated disordered systems.**
- **The degree of hyperuniformity provides an order metric for the extent to which large-scale density fluctuations are suppressed in such systems.**
- **Disordered hyperuniform systems appear to be endowed with unusual physical properties that we are only beginning to discover.**
- **Directional hyperuniform materials represents an exciting new extension.**
- **Hyperuniformity has connections to physics and materials science (e.g., ground states, quantum systems, random matrices, novel materials, etc.), mathematics (e.g., geometry and number theory), and biology.**

CONCLUSIONS

- Disordered hyperuniform materials are new ideal states of disordered matter.
- Hyperuniformity provides a unified means of categorizing and characterizing crystals, quasicrystals and special correlated disordered systems.
- The degree of hyperuniformity provides an order metric for the extent to which large-scale density fluctuations are suppressed in such systems.
- Disordered hyperuniform systems appear to be endowed with unusual physical properties that we are only beginning to discover.
- Directional hyperuniform materials represents an exciting new extension.
- Hyperuniformity has connections to physics and materials science (e.g., ground states, quantum systems, random matrices, novel materials, etc.), mathematics (e.g., geometry and number theory), and biology.

Collaborators

Robert Batten (Princeton)
Paul Chaikin (NYU)
Joseph Corbo (Washington Univ.)
Marian Florescu (Surrey)
Miroslav Hejna (Princeton)
Yang Jiao (Princeton/ASU)
Gabrielle Long (NIST)
Etienne Marcotte (Princeton)
Weining Man (San Francisco State)
Sjoerd Roorda (Montreal)
Antonello Scardicchio (ICTP)
Paul Steinhardt (Princeton)
Frank Stillinger (Princeton)
Chase Zachary (Princeton)
Ge Zhang (Princeton)